Three-dimensional finite element analysis of braced excavation systems

Winata, Berlina Margaretha.

2010

Winata, B. M. (2010). Three-dimensional Finite Element Analysis of Braced Excavation Systems. Final year project report, Nanyang Technological University.

https://hdl.handle.net/10356/91546

GE-17:
THREE-DIMENSIONAL FINITE ELEMENT ANALYSIS OF BRACED EXCAVATION SYSTEMS

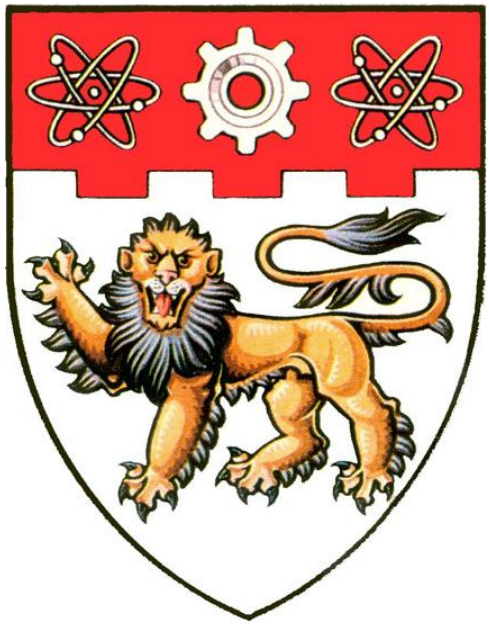

BERLINA MARGARETHA WINATA

SCHOOL OF CIVIL AND ENVIRONMENTAL ENGINEERING
COLLEGE OF ENGINEERING
NANYANG TECHNOLOGICAL UNIVERSITY

2009

GE-17:
THREE-DIMENSIONAL FINITE ELEMENT ANALYSIS OF BRACED EXCAVATION SYSTEMS

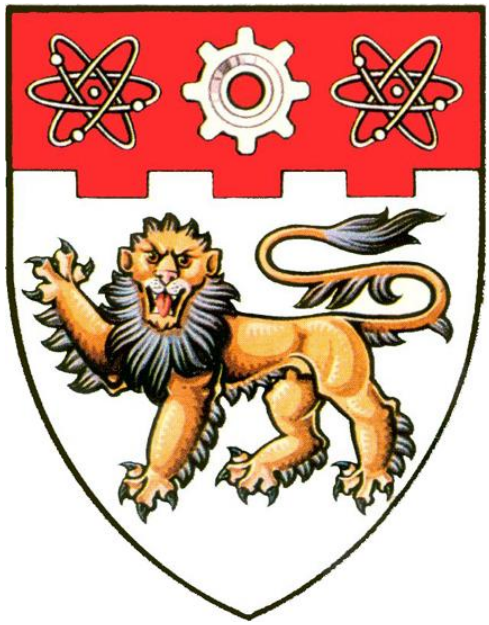

Submitted by:

BERLINA MARGARETHA WINATA

School of Civil and Environmental Engineering
College of Engineering
Nanyang Technological University

A Final Year Project presented to the Nanyang Technological University
in partial fulfillment of the requirements for the
Degree of Bachelor of Engineering

2010

ACKNOWLEDGEMENTS

The author would like to express her sincere gratitude to individuals who have given tremendous helps and supports during the completion of this project:

Firstly, the author would like to express her appreciation to Associate Professor Anthony Goh Teck Chee. His suggestions, guidance, and comments throughout the entire project have led to the author's better understanding on the project.

The author would also like to thank the staffs from CADD Lab II for making necessary arrangements to support the completion of the author's study in the computer lab.

Lastly, the author wishes to thank her family and friends for their support and care throughout the period of study.

ABSTRACT

Braced excavation study is usually modeled using plane strain (two-dimensional) finite element analysis. In this kind of analysis, the length of excavation wall is assumed to be infinitely long, so that the effect of the length of excavation is neglected. However this analysis may not correctly represent the actual scenario of the braced excavation system, especially for the excavation in which the wall length is short.

In this report, a three-dimensional finite element parametric study which includes 24 finite element simulations with varied excavation length and wall system stiffness is conducted to examine the effect of excavation geometry on the performance of braced excavation system in a typical Singapore soft clay soil profile. The aspects that are examined are the wall lateral movements, bending moments, lateral earth pressure and strut loads. In addition, analyses were also carried out to study the distribution of strut forces after the failure of the lowest strut.

Comparisons between plane strain and three-dimensional analyses are carried out in terms of the plane strain ratio (PSR). PSR is defined as the ratio of maximum lateral movement behind the primary wall between plane strain and three-dimensional finite element analyses.

The results show that for flexible and medium flexible walls, when the ratio of excavation length to the excavation height and to the excavation width is greater than 3 and 2.5 respectively, the wall lateral movements from three-dimensional analysis agree with the results from plane strain analysis provided that the excavation height and width are constant. However no clear conclusions can be drawn for the case of stiff walls. The results also show that majority portion of the failed strut force is distributed to other adjacent struts instead of only to the strut immediately above it as assumed in plane strain analysis.

TABLE OF CONTENTS

ACKNOWLEDGEMENTS……i

ABSTRACT.....ii

TABLE OF CONTENTS……..iii

LIST OF TABLES……..v

LIST OF FIGURES……...vi

LIST OF SYMBOLS……...viii

Chapter 1: Introduction

1.1 Research Background……...……1

1.2 Objectives……...…….....2

1.3 Scope of Work……...……2

1.4 Organization……...2

Chapter 2: Literature Review

2.1 Earth Pressure Distribution in Braced Excavation in Clay.....…...4

2.2 Factors Affecting Performance of Braced Excavation……...7

2.2.1 Excavation Shape……..7

2.2.2 Soil Characteristic……8

2.2.3 Support System Stiffness…….....9

2.3 Lateral Wall Movements in Braced Excavation……..…….....10

2.4 Mohr-Coulomb Soil Model for Clay……12

Chapter 3: Methodology

3.1 Plane Strain Problem.....…….....14

3.2 Three-dimensional Problem……15

3.3 Mohr-Coulomb Model in Finite Element Analysis……..15

3.4 Parametric Study……...…...16

3.4.1 Soil Parameters……...……18

3.4.2 Support System Parameters……...…….19

3.4.3 Excavation Stages……...……23
3.4.4 Plaxis Models for the Parametric Study……..24

Chapter 4: Results and Analyses

4.1 Lateral Movements of the Primary Wall – General Trends……..……27
4.1.1 Effects of Excavation Size……..30
4.1.2 Effects of Wall Stiffness……..…...31
4.2 Bending Moments of the Primary Wall……...……...……....32
4.3 Lateral Earth Pressure……..34
4.4 Strut Loads and Apparent Pressure Diagram……...35
4.5 Lateral Movements of the Secondary Wall…….…...……..……37
4.6 Strut Failure Condition…….39
4.6.1 Lateral Movements of the Primary Wall after Failure…….……...39
4.6.2 Lateral Earth Pressure after Failure...…….40
4.6.3 Distribution of Strut Forces……41

Chapter 5: Conclusions and Recommendations

5.1 Conclusions……..45
5.2 Recommendations……46

REFERENCES……..…47

Appendix A…….…….…..50
Appendix B…….……..53
Appendix C…..…….……62
Appendix D…….……...……...72
Appendix E…….……...78
Appendix F…….……...82
Appendix G…….…….....88
Appendix H……...……...97
Appendix I……...……...103

LIST OF TABLES

Table No.	Descriptions	Page
3.1	Cases with Varying Excavation Length	18
3.2	Material Properties for the Soil Layers	19
3.3	Wall Stiffness Parameters for Plane Strain and Three-dimensional Analysis	22
3.4	Struts Parameters for Plane Strain Analysis	22
3.5	Waler and Struts Parameters for Three-dimensional Analysis	22
3.6	Excavation Stages for Plane Strain and Three-dimensional Analyses	23
4.1	Maximum Lateral Movements of Primary Wall	29
4.2	Maximum Lateral Movements of Primary Wall: Before and After Strut Failure	39
4.3	Percentages of Strut Forces Distribution after Lowest Strut Failure	43

LIST OF FIGURES

Figure No.	Descriptions	Page
2.1	Theoretical Active Earth Pressure Acting Behind Wall	4
2.2	Pressure Distribution Profile in Braced Excavation	5
2.3	Terzaghi and Peck's (1967) APD for Soft to Medium Clay	5
2.4	Terzaghi and Peck's (1967) APD for Stiff Clay	6
2.5	Corner Effect on Wall Movement (Bono et al., 1992)	8
2.6	Effect of Soil Shear Strength on Lateral Wall Movements (Wong and Broms, 1989)	9
2.7	Effect of Wall System Stiffness on Lateral Wall Movements (Clough et al., 1989)	10
2.8	Terzaghi's Factor of Safety against Basal Heave versus Maximum Wall Movements (Mana and Clough, 1981)	10
2.9	Strut Stiffness Factor versus Maximum Wall Movements (Mana and Clough, 1981)	11
2.10	Clay Modulus Factor versus Maximum Wall Movements (Mana and Clough, 1981)	11
2.11	Effect of Wall Depth on Wall Movements (Wong and Broms, 1989)	12
2.12	Effect of Wall Width on Wall Movements (Wong and Broms, 1989)	12
2.13	Overconsolidation Ratio versus E_u / c_u (Dincan and Buchigani, 1976)	13
3.1	Typical Stress-Strain Behavior in Material	15
3.2	Stress-Strain Curve of Perfectly Plastic Model	16
3.3	Soil Profile Used for the Parametric Study	17
3.4	Plan View of the Strut Arrangement	17
3.5	Definition of a Wall's Local System of Axes and Various Quantities	21
3.6	Local System Axes Definition of Moment of Inertia (I) and Positive Bending Moment (M) for a Horizontal Beam	21
3.7	Typical Mesh of Plane Strain Model	25

3.8	Typical Three-dimensional Mesh of Three-dimensional Model	25
3.9	Typical Deformed Mesh of Plane Strain Model	26
3.10	Typical Deformed Mesh of Three-dimensional Model	26
4.1	Lateral Movements of Primary Wall of Cases A, B and C	28
4.2	Maximum Lateral Movements of Primary Wall	29
4.3	Effect of Excavation Size to PSR	30
4.4	Wall Bending Moments of Cases A, B and C	33
4.5	Maximum Wall Bending Moments of Cases A, B and C	34
4.6	Lateral Earth Pressure Diagram for Cases of Flexible Wall	34
4.7	Comparison between Pressure Diagrams from Plaxis Analyses and from Terzaghi-Peck's APD	36
4.8	Lateral Movements of Secondary Wall of Cases A, B and C	38
4.9	Earth Pressure Diagram for Cases of Flexible Wall after Strut Failure	40
4.10	Elevation View of Struts Arrangement in Primary Wall	41
4.11	Percentage of Strut Forces Distributed to Adjacent Struts after Strut Failure	42
4.12	Total Percentage of Strut Forces Distributed to the Immediate Adjacent Struts after Lowest Strut Failure	43

LIST OF SYMBOLS

Symbol	Description	SI Unit
A	Area	m^2
B	Width	m
c	Cohesion	kPa
c_u	Undrained cohesion	kPa
E	Young's modulus	kPa
E_i	Initial tangent modulus	kPa
E_u	Undrained Young's modulus	kPa
E_{50}	Elastic stiffness of clay and silt at 50% of failure stress	kPa
H_e	Height of excavation	m
h	Average vertical spacing of lateral support element or struts	m
I	Moment of inertia	$kg.m^2$
K_o	Coefficient of lateral earth pressure at rest	unitless
k	Stiffness coefficient	unitless
L	Length	m
N_{SPT}	SPT blow count	blows/300 mm
P	Force applied to the body	kN
z	Depth of excavation	m
γ	Unit weight	kN/m^3
γ_w	Unit weight of water	kN/m^3
δ	Total deflection	m
$\delta_{\max}$	Maximum deflection	m
ν	Poisson's ratio	unitless
σ_a	Active lateral pressure from Peck's Apparent Pressure Diagram	kPa

φ	Friction angle	^{o}
ψ	Dilatancy angle	^{o}

CHAPTER 1
INTRODUCTION

1.1 Research Background

Almost all of excavation projects nowadays utilize geotechnical finite element software to model the excavation and foundation design. One of the widely used softwares for this purpose is the Plaxis program.

Braced excavation comprises an excavation project which is braced in a certain direction by struts to prevent the soil cave-in. Majority of braced excavation analyses assume a plane strain condition, ie. the length of the excavation wall is assumed to be infinitely long, and thus analyses are performed two-dimensionally. However this two-dimensional analysis may not correctly represent the actual soil movements, especially for the excavation in which the wall length is considered short (ie, the ratio of length to height of excavation is small).

In this kind of excavation, plane strain analysis neglects the corner stiffening effect which may lead to smaller ground movements near the corners, and larger ground movements toward the middle of excavation wall (Finno et al., 2007).

In this project, three-dimensional finite element analysis will be used to simulate and analyze such conditions for a fairly thick soft clay stratum typical of some areas in Singapore. The analyses are intended to investigate the effects of excavation length and wall stiffness on the performance of braced excavation system.

This study involves comparison between plane strain and three-dimensional finite element analysis results in terms of lateral wall movements, and consequently, wall bending moments, lateral earth pressure and strut loads. Twenty four cases are performed, which include cases of varying excavation length and wall stiffness for plane strain and three-dimensional analyses. In addition, cases of one strut failure condition were also considered.

1.2 Objectives

The objectives of this project are to compare and highlight the difference in the performance of braced excavation system in plane strain and three-dimensional finite element analyses, including in the cases of one strut failure; and to propose general guidelines in which three-dimensional analysis is more appropriate than plane strain analysis.

1.3 Scope of Work

The scope of work includes modeling and case analysis of both plane strain and three-dimensional finite element braced excavation cases with varying excavation length and wall stiffness applied to typical Singapore soft clay soil stratum. Plane strain and three-dimensional analysis results are to be compared in terms of lateral wall movements due to excavation, wall bending moments, lateral earth pressure and strut loads.

Modeling and case analysis also include comparisons between plane strain and three-dimensional analysis for one strut failure condition.

1.4 Organization

This report is divided into five chapters. The scopes of respective chapters are as follows:

Chapter 1 covers the information about braced excavation system and the application of finite element analysis on braced excavation studies. The objectives and scopes of the project are also highlighted.

Chapter 2 provides literature review on the various aspects in braced excavation system including factors affecting performance of braced excavation system.

Chapter 3 consists of explanations about the finite element method and techniques for simulating the behavior of braced excavation system. The information of parametric studies used in this project is also introduced.

Chapter 4 presents the results of the parametric study from plane strain and three-dimensional finite element analyses. Comparisons between the results of plane strain and three-dimensional analyses are presented.

Chapter 5 consists of general conclusions and recommendations based on the results of parametric study conducted.

Details of the results from the parametric study are presented in Appendix.

CHAPTER 2

LITERATURE REVIEW

2.1 Earth Pressure Distribution in Braced Excavation in Clay

A typical braced excavation system consists of a flexible or stiff retaining wall, horizontal walers and struts or ground anchors. Horizontal struts are used as temporary bracing system to maintain stability. The most common wall types in Singapore are sheet piles, bored piles and diaphragm walls. After wall installation, walers and struts are installed in stages as excavation proceeds.

In a typical gravity-type retaining wall, lateral earth pressure, or horizontal stress in soil in the active condition can be determined by general wedge theories in which earth pressure distribution acting behind the wall is triangular, as shown in *Figure 2.1* below.

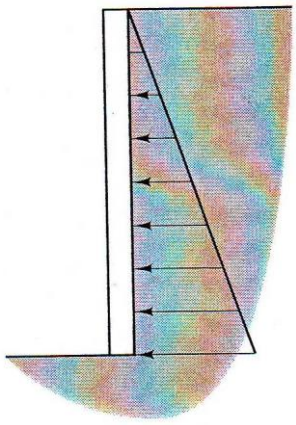

Figure 2.1: Theoretical Active Earth Pressure Acting Behind Wall.

However, the typical pressure distribution profile developed during braced excavation is different, as shown in *Figure 2.2*. The behavior of lateral pressure does not satisfy the general wedge theory where the lateral pressure is increasing hydrostatically. The complexity of lateral pressure distribution in braced excavation is contributed by several factors such as the type of soil, the construction method, the strut installation, and type of equipment used.

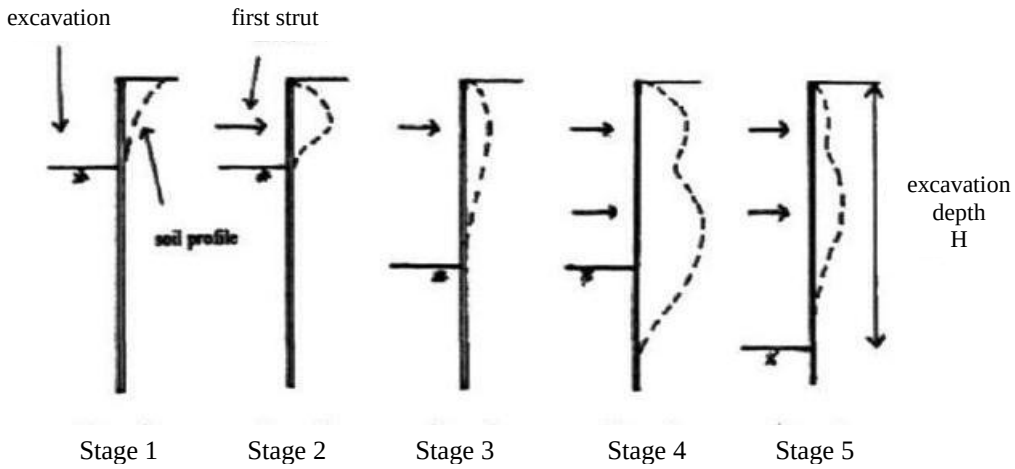

Figure 2.2: Pressure Distribution Profile in Braced Excavation

Due to the difficulty in measuring the actual soil pressure in braced excavation, simplified methods to determine pressure distribution are commonly utilized. Terzaghi and Peck (1967) proposed the apparent earth pressure diagrams, herein referred to as APD, to calculate the strut loads on braced excavations. The APD are semi-empirical in nature, being based on actual measurements of strut loads in braced excavations with relatively flexible walls. These diagrams are not intended to represent the real distribution of earth pressure at any vertical section in an excavation, but instead they represent the upper bound of all measurements (Peck, 1969). Terzaghi and Peck proposed the pressure diagram in *Figure 2.3* below for cuts in soft to medium clay.

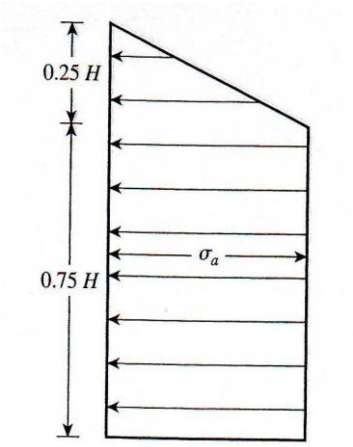

Figure 2.3: Terzaghi and Peck's (1967) APD for Soft to Medium Clay

Behavior of braced excavation in clay depends on the stability number $\gamma H_e / c_u$. The pressure diagram in *Figure 2.3* is only applicable when stability number is greater than 4. The pressure σ_a can then be derived from the equation below,

$$\sigma_a = \gamma H_e \left[1 - m \frac{4c_u}{\gamma H_e} \right] \tag{2.1}$$

where γ is unit weight of excavated soil, H_e is excavation depth and c_u is the undrained cohesion ($\varphi = 0$). For deep deposit of soft clay, the value of $m = 0.4$ is used, otherwise the value is taken as $m = 1$. The value that gives the larger σ_a is adopted in design.

In the case where stability number is less than 4, Terzaghi and Peck suggested the pressure diagram in *Figure 2.4* to be used. This pressure diagram mainly applies for cuts in stiff clay.

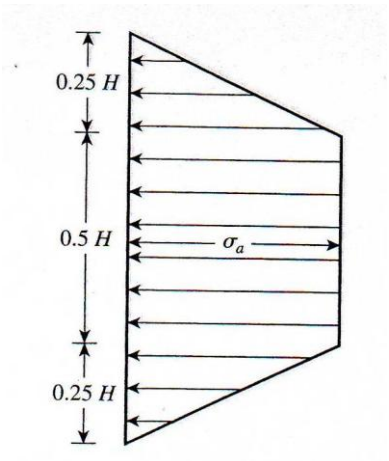

Figure 2.4: Terzaghi and Peck's (1967) APD for Stiff Clay

The value of σ_a can be calculated from the equation below:

$$\sigma_a = 0.2\gamma H_e \text{ to } 0.4\gamma H_e \tag{2.3}$$

Clay is assumed to be undrained and total stress analysis is considered, as the period of excavation is assumed to be short.

Even though Terzaghi and Peck's APD have been widely used in practice, the applicability of using these diagrams for diaphragm wall is still uncertain. Chang and Wong (1996) studied the application of Terzaghi and Peck's APD on diaphragm walls particularly in soft clay. The study concluded that Terzaghi and Peck's APD tend to underestimate the strut forces when the ratio of E_i / c_u falls below 500; where E_i is the initial tangent modulus and c_u is the undrained shear strength. It is observed that when E_i / c_u ratio falls between 200 to 500, except for the lowest strut, the APD underestimate the strut forces by as much as 100%. As the E_i / c_u ratio increases to 1000, Terzaghi and Peck's APD become more applicable (Chang and Wong, 1996).

In this study, the E_i / c_u ratio utilized is 300 and 400 for soft and stiff clay respectively. Therefore, underestimation of strut forces by APD is expected.

2.2 Factors Affecting Performance of Braced Excavation

When a layer of soil is excavated, the stress and strains within the soil mass will change. Ground movements will occur, which will lead to lateral wall movements. Ground movement in braced excavation is influenced by many factors, such as dimension of excavation, soil characteristic, support system stiffness, construction procedure, and workmanship. The first three factors will be discussed below.

2.2.1 Excavation Shape

The corner of the excavation wall is stiffer due to the intersection of two walls which restrain each other's movements. Bono et al. (1992) reported that the corner of excavation will cause significant reduction in lateral movements and ground settlement, as shown in *Figure 2.5*. Other reports by Ou et al. (1996) and Lee et al. (1998) reported similar results. Finno et al. (2007) investigated this corner stiffening effect by comparing lateral wall movements of plane strain and three-dimensional finite element analyses, and concluded that as the length of excavation increases, the corner effect diminishes.

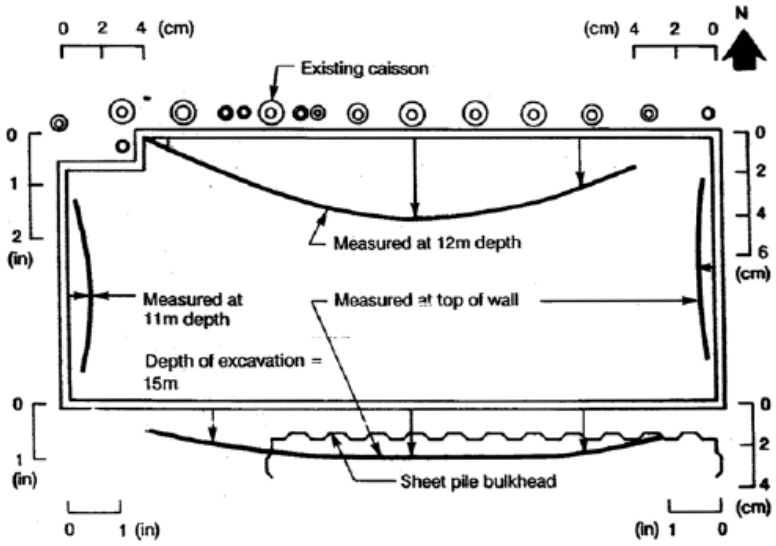

Figure 2.5: Corner Effect on Wall Movement (Bono et al., 1992)

Investigation by Finno et al. (2007) also concluded that corner stiffening effect depends on length to height (L/H_e) and length to width (L/B) ratio, support system stiffness and factor of safety against basal heave.

2.2.2 Soil Characteristics

Wong and Broms (1989) investigated the effect of undrained shear strength on lateral wall movements using finite element analysis. The result shown in *Figure 2.6* indicates that as soil strength (c_u) increases, the lateral wall movements decrease. When the factor of safety against basal heave is greater than 2, the change in wall movements is small.

Soil stiffness also contributes in lateral wall movements, as higher soil stiffness results in smaller movements. Soil stiffness factor is crucial to lateral wall movements, especially in the case where factor of safety against basal heave is less than 1.5 (Clough et al., 1977).

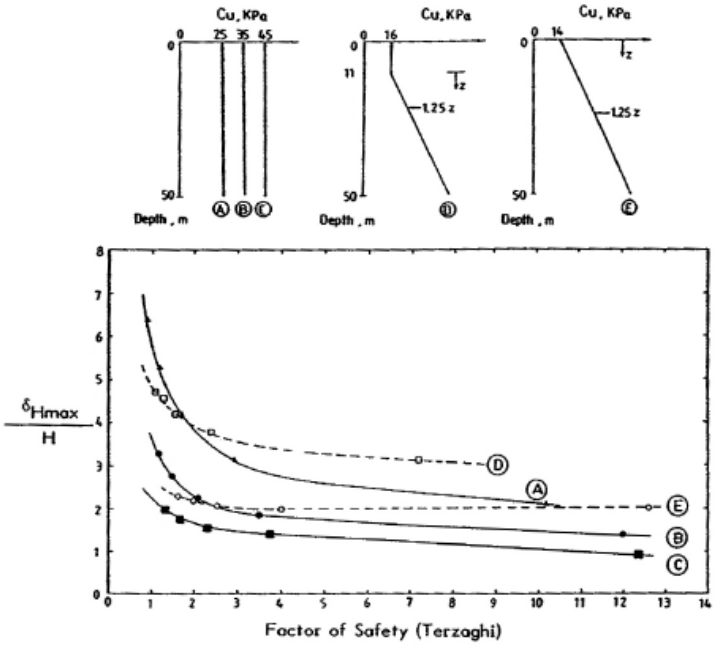

Figure 2.6: Effect of Soil Shear Strength on Lateral Wall Movements (Wong and Broms, 1989)

2.2.3 Support System Stiffness

In braced excavation, support system includes wall, walers, struts, rakers and ground anchors. Clough et al. (1989) defined wall system stiffness as $EI / \gamma_w h^4$; where EI is the wall stiffness, γ_w is the unit weight of water, and h is the average vertical spacing of lateral support elements or struts. *Figure 2.7* shows the effect of wall system stiffness on wall movements. In general, lateral wall movements decrease as the wall system stiffness increases. This effect is amplified in cases where factor of safety is less than 1.5.

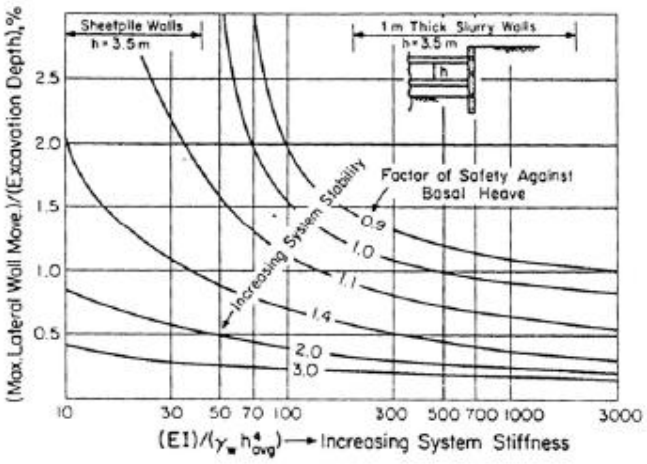

Figure 2.7: Effect of Wall System Stiffness on Lateral Wall Movements (Clough et al., 1989)

2.3 Lateral Wall Movements in Braced Excavation

Mana and Clough (1981) investigated the lateral wall movements based on finite element analysis. Mana and Clough (1981) related the lateral wall movements to a coefficient of correction for system stiffness, which takes into account the effect of wall and strut stiffness, depth to firm layer, and excavation width. Other than that, lateral wall movements also depend on Terzaghi's factor of safety against basal heave, strut preloading factor, and clay modulus factor, as shown in *Figures 2.8, 2.9* and 2.*10*.

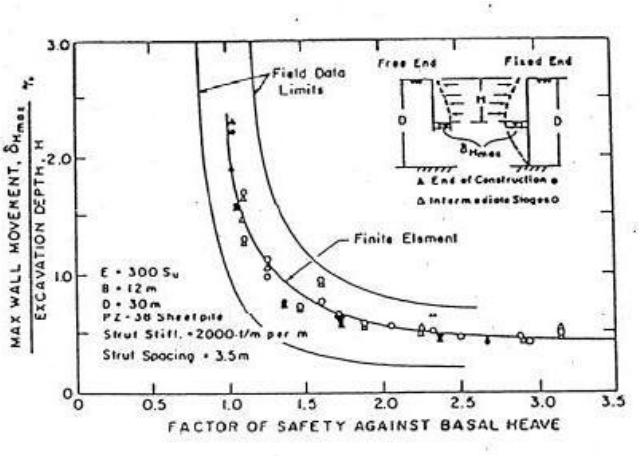

Figure 2.8: Terzaghi's Factor of Safety against Basal Heave versus Maximum Wall Movements (Mana and Clough, 1981)

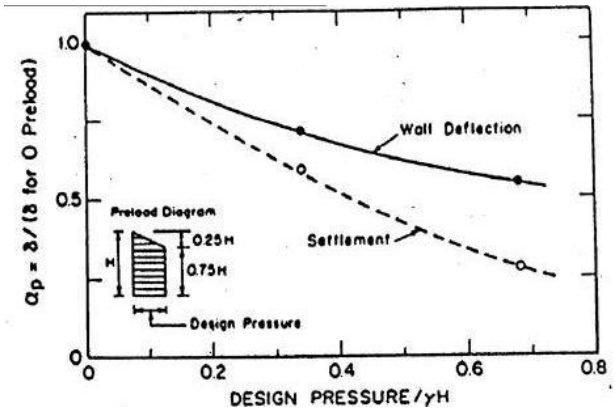

Figure 2.9: Strut Stiffness Factor versus Maximum Wall Movements (Mana and Clough, 1981)

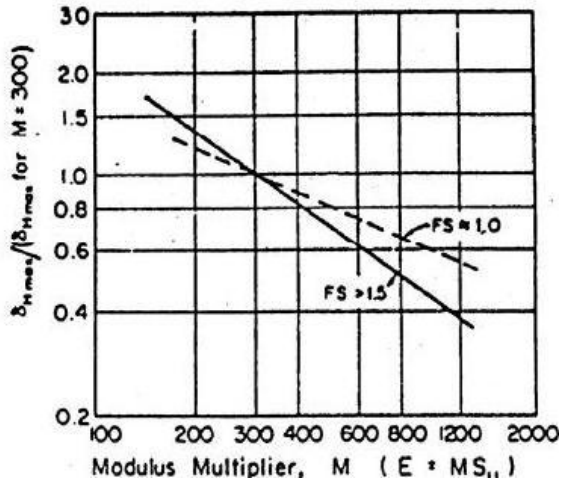

Figure 2.10: Clay Modulus Factor versus Maximum Wall Movements (Mana and Clough, 1981)

Wong and Broms (1989) also investigated the lateral wall movements in relation with depth and width of excavation. As excavation progresses deeper, the lateral movements increase, due to reduction in factor of safety against basal heave along the depth. The effects of depth and width on lateral wall movements are shown in *Figure 2.11* and *Figure 2.12*.

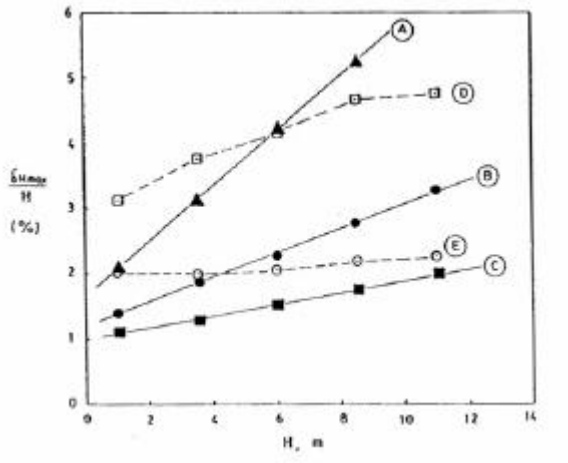

Figure 2.11: Effect of Wall Depth on Wall Movements (Wong and Broms, 1989)

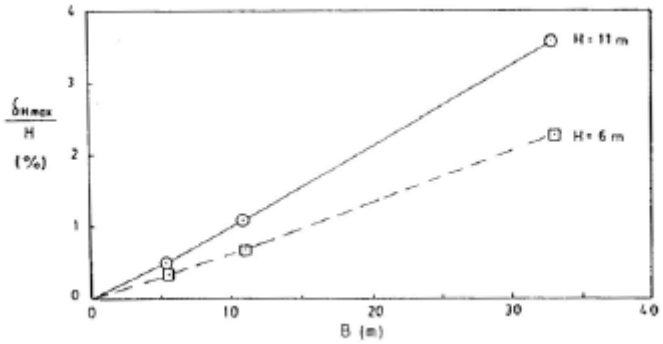

Figure 2.12: Effect of Wall Width on Wall Movements (Wong and Broms, 1989)

2.4 Mohr-Coulomb Soil Model for Clay

Assessment on ground and wall movement predictions relies on accuracy of soil model used in the investigation. Mohr-Coulomb model is widely used for Singapore soil conditions, due to its simplicity.

Elastic stiffness of clay and silt at 50% of the failure stress (E_{50}) can be determined from the chart by Duncan and Buchigani (1976) shown in *Figure 2.13*. In this study, undrained Young's modulus (E_u) equals $300\,c_u$ is adopted for soft clay, and (E_u) equals $400\,c_u$ is adopted for stiff clay.

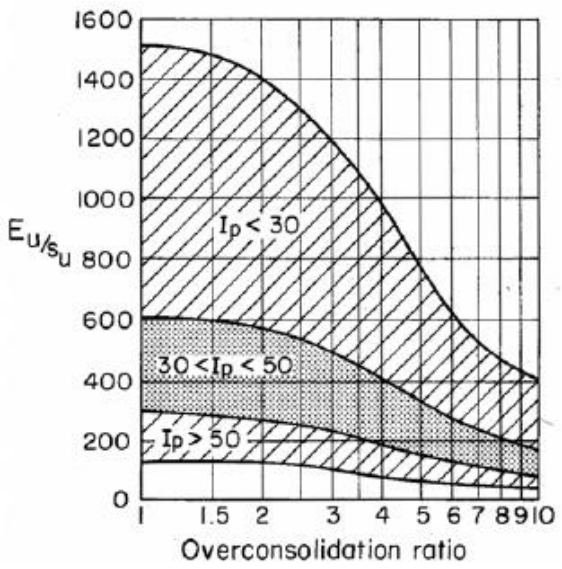

Figure 2.13: Overconsolidation Ratio versus E_u / c_u (Duncan and Buchigani, 1976)

Value of undrained shear strength is also related to the standard penetration blowcount (N_{SPT}) value. Stroud (1974) suggested that c_u is between the ranges of 4 to 6 N_{SPT}.

CHAPTER 3

METHODOLOGY

Finite element analysis involves breaking down a set of domain into many smaller parts to obtain approximate solutions of each part. The solution from each part is then assembled to obtain the solution of whole domain. In this study, finite element analysis softwares Plaxis Version 8 and Plaxis 3D Foundation are used for plane strain analysis and three-dimensional analysis respectively.

Mohr-Coulomb model for undrained analysis is used for the soil. Mohr-Coulomb model can be simulated by two ways. The first is by adopting total stress approach by using total stress parameter (c_u, φ_u, E_u and $\nu = 0.495$). The second way is by adopting effective stress analysis using effective stress parameters ($c', \varphi', E' = 0.9E_u$ and $\nu' = 0.33$). For undrained analysis involving soft clay, the first option can produce reliable results, while the second option may produce erroneous results (Wong, 2003 & 2004). Therefore, the first option is adopted for this study.

The excavation is simulated by 'stage construction', where structural elements can be activated or deactivated to simulate the excavation or construction sequence.

More details on the finite element method and how it simulates the excavation process are explained in *Appendix A*.

3.1 Plane Strain Problem

Plane strain problem in this report refers to two-dimensional analysis. Typical geotechnical structures such as retaining walls, continuous footings and slopes generally have one dimension (ie. length) very large in comparison with the other two. The z-dimension is usually assumed to be greater than x and y dimension. As the result, the strain in the direction of z-axis can be assumed to be zero, and displacements in x and y planes are independent of the z coordinate. The numerical integration along the z-axis is performed for a unit section (1 unit length).

When performing plane strain analysis, the stresses considered are only σ_x, σ_y and τ_{xy}. Since, the problem is reduced to only two axes, the solution time is considerably faster.

3.2 Three-dimensional Problem

While many cases can be simplified to plane strain analysis, in reality there are some problems which must be treated as three-dimensional. Instead of analyzing two-dimensional section of original geometry, the whole domain is considered. The whole domain will be represented by three-dimensional finite elements.

As all three dimensions are taken into account in the analysis, three-dimensional analysis involves considerably more elements, nodes, and solution time as compared to plane strain analysis.

3.3 Mohr-Coulomb Model in Finite Element Analysis

In the modeling of soil, several stress-strain behaviors are assumed. Typical models are shown in *Figure 3.1* below.

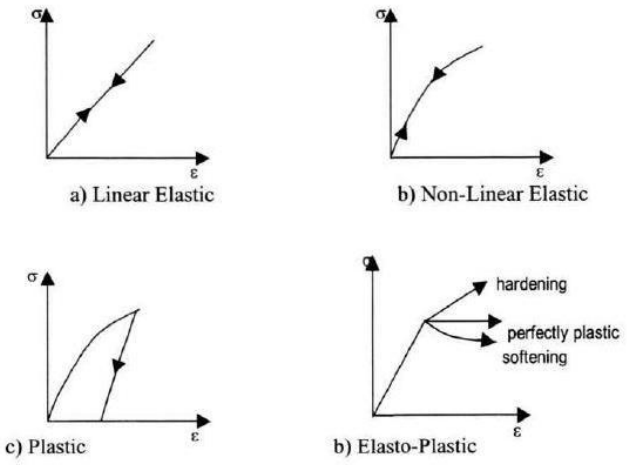

Figure 3.1: Typical Stress-Strain Behavior in Material

In finite element analysis, soil behavior is mostly modeled as elasto-plastic, including for Mohr-Coulomb model, which is modeled as perfectly plastic model. A perfectly plastic model is a constitutive model with a fixed yield surface. This characteristic is illustrated in *Figure 3.2* below.

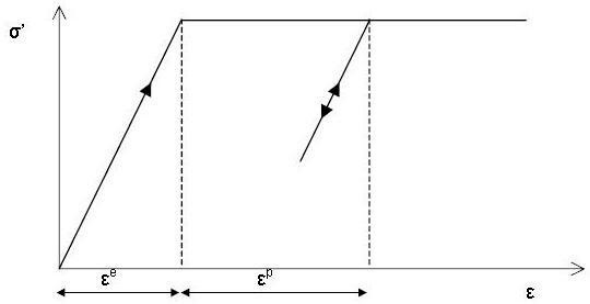

Figure 3.2: Stress-Strain Curve of Perfectly Plastic Model

Mohr-Coulomb model only requires five input parameters, including Young's modulus (E), Poisson's ratio (ν), friction angle (φ), cohesion (c) and dilatancy angle (ψ). Three of these, c, φ and ψ control the plastic behavior while the other two, E and ν control the elastic behavior. Mohr-Coulomb model does not include small strain non-linearity effect.

3.4 Parametric Study

The soil stratum used in the analyses is typical of a Singapore soft clay soil profile underlain by stiffer clay layers, as shown in *Figure 3.3*.

The excavation depth (H_e) is 16 m, excavation width (B) is 20 m, and the wall embedment depth is 4 m. The top 20 m comprises a soft-medium clay layer, followed by a 6 m of stiff clay layer, and a 10 m of stiffer clay layer to the hard stratum. Since the total stress analysis is carried out, the ground water table is ignored.

In this report, the wall along the length (L) is referred to as the primary wall, and the wall along the excavation width (B) is referred to as the secondary wall. Effects of excavation on the primary wall are more critical because of its greater dimension as compared to the secondary wall. Two kinds of strut are installed. Primary struts are installed along the width of the excavation, and secondary struts are installed along the length of the excavation, as can be

seen in *Figure 3.4*. Both primary and secondary struts are installed in five layers with horizontal spacing of 5 m, and vertical spacing ranging from 2 m to 3 m. Secondary struts are installed 0.5 m below the primary struts. For plane strain analysis, only primary struts can be modeled. In this study, only primary struts are of interest.

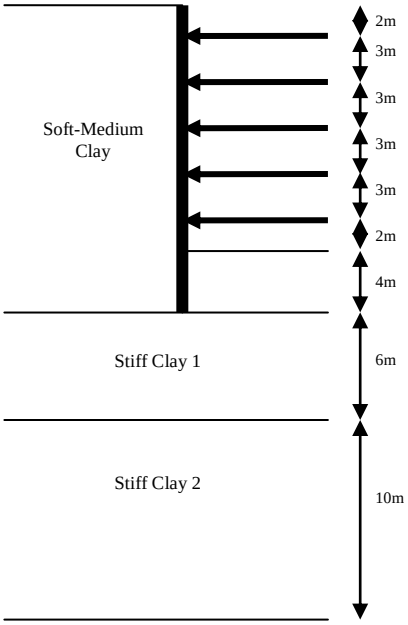

Figure 3.3: Soil Profile Used for the Parametric Study

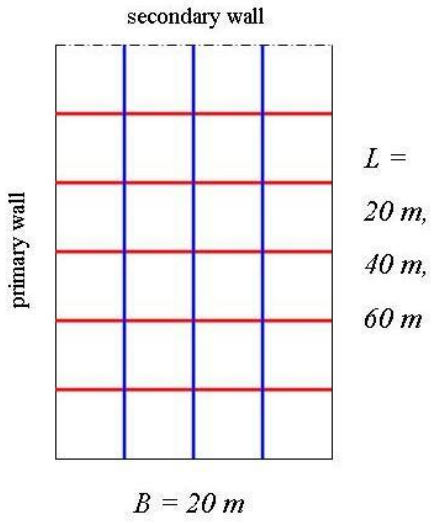

Figure 3.4: Plan View of the Strut Arrangement. Red lines indicate the primary struts, blue lines indicate the secondary struts.

For the plane strain analysis, only the variation of the support system stiffness can be simulated. Therefore plane strain analysis only considers cases of different wall stiffness, namely Case A for flexible wall, Case B for medium wall and Case C for stiff wall. However for three-dimensional analysis, varying excavation length can also be modeled together with varying support system stiffness. Cases 1, 2 and 3 consider the excavation length as an independent variable. Each of these cases will be analyzed for flexible, medium and stiff wall support condition, as shown in *Table 3.1*. All of the cases above are also modeled for their respective one strut failure condition.

Table 3.1: Cases with Varying Excavation Length

Case	Analysis	Depth (m)	Width (m)	Length (m)	Embedment Depth (m)	L/H_e	L/B
A, B, C	2D	16	20	-	4	-	-
1A, B, C	3D	16	20	20	4	1.25	1
2A, B, C	3D	16	20	40	4	2.5	2
3A, B, C	3D	16	20	60	4	3.75	3

3.4.1 Soil Parameters

The soil profile consists of a thick layer of soft clay, extending down to the depth of 20 m. The undrained shear strength (c_u) for this layer is assumed to increase linearly with the depth so that $c_u = 20 + 1.2z$, where z is the depth of excavation below the original ground surface. Undrained elastic modulus (E_u) equals to 300 c_u is adopted, and consequently, E_u also increases linearly with depth.

Underlying the soft clay layer are two layers of stiff clay. The undrained shear strengths are 150 kPa and 500 kPa respectively. These values are constant along each layer's depth. For both layers, E_u = 400 c_u is adopted. For all soil layers, coefficient of lateral earth pressure at rest (K_o) is taken as 1, friction angle (φ) and dilatancy angle (ψ) are both zero, and undrained (total stress) analysis is carried out.

Material data sets for the soil layers are tabulated in *Table 3.2* below.

Table 3.2: Material Properties for the Soil Layers

Mohr-Coulomb			**Soft-Medium Clay**	**Stiff Clay 1**	**Stiff Clay 2**
Parameter	**Name**	**Unit**	Drained	Drained	Drained
Unsaturated soil unit weight	γ_{unsat}	kN/m³	16	16	16
Saturated soil unit weight	γ_{sat}	kN/m³	18	18	18
Permeability in x-dir	k_x	m/day	0	0	0
Permeability in y-dir	k_y	m/day	0	0	0
Elastic Modulus	E_{ref}	kN/m²	6000	60000	200000
Poisson's ration	υ	-	0.495	0.495	0.495
Cohesion	c_{ref}	kN/m²	20	150	500
Friction angle	φ	°	0	0	0
Dilatancy angle	ψ	°	0	0	0
Increment of E	E_{inc}	kN/m²	360	0	0
Increment of c	$c_{increment}$	kN/m²/m	1.2	0	0
Interface reduction factor	R_{inter}	-	1	1	1
Interface permeability			Neutral	Neutral	Neutral

3.4.2 Support System Parameters

Support system for plane strain analyses includes wall and struts. For three-dimensional analyses, walers are added as additional support element.

Plane strain simulations represent wall and lateral support stiffness on per length unit basis, and therefore ignore the effect of waler between wall and struts. In three-dimensional analysis, the presence of waler is simulated. The walers basically transfer the earth pressure from the wall to the struts.

The wall system stiffness, S (Clough et al., 1989) is used to represent the flexibility of the wall, and can be computed using the equation below,

$$S = \frac{EI}{\gamma_w h^4} \tag{3.1}$$

where EI is the bending stiffness of the wall, h is the average vertical spacing of lateral support elements and γ_w is the unit weight of water.

When modeling three-dimensional cases, care must be taken in defining the stiffness parameters of the structural elements, due to the addition of one axis z. Instead of only requiring one input, three-dimensional analysis requires three stiffness parameters to represent the axes.

For wall element, E_1, E_2 and E_3 represent the Young's modulus in first, second and third axial direction, respectively. G_{12} represents the in-plane shear modulus. G_{13} and G_{23} represent out-of-plane shear modulus related to shear deformation over first and second direction, respectively. The local system of axes is shown in *Figure 3.5*.

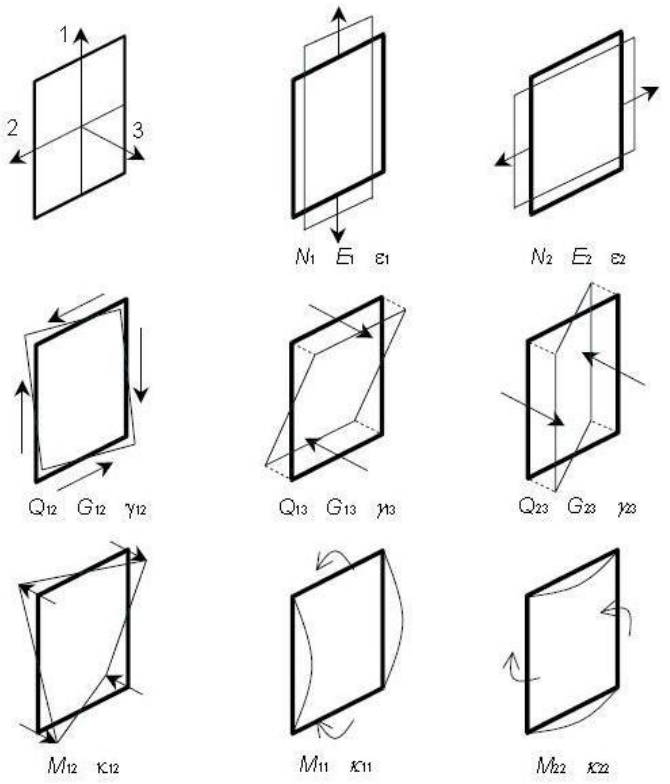

Figure 3.5: Definition of a Wall's Local System of Axes and Various Quantities

For the beam element, the linear beam stiffness requires the input of Young's Modulus and three moments of inertia: I_2, I_3 and I_{23}. I_2 and I_3 represent the moments of inertia against bending around the second and third axes, respectively. I_{23} represents the moment of inertia against oblique bending, and the value is zero for symmetric beam profiles. *Figure 3.6* shows the local system of axes for a horizontal beam.

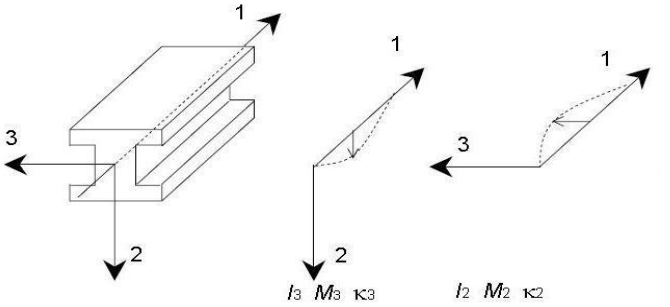

Figure 3.6: Local System Axes Definition of Moment of Inertia (I) *and Positive Bending Moment* (M) *for a Horizontal Beam*

Material properties for the support systems are tabulated in *Tables 3.3, 3.4 and Table 3.5* below.

Table 3.3: Wall Stiffness Parameters for Plane Strain and Three-dimensional Analysis

Parameter	**Name**	**Unit**	**Wall**		
			Flexible	**Medium**	**Stiff**
Plane strain parameters					
System stiffness	S	-	32	320	3,200
Bending stiffness	EI	kNm^2/m	50,400	504,000	5,040,000
Axial stiffness	EA	kN/m	3,427,000	34,270,000	342,700,000
Element thickness	d	m	0.42	0.42	0.42
Poisson's ratio	ν	-	0	0	0
Three-dimensional parameters					
Young's modulus	E_1	kPa	8,160,000	81,600,000	816,000,000
	E_2	kPa	408,000	4,080,000	40,800,000
	E_3	kPa	200,000,000	2,000,000,000	20,000,000,000
Shear modulus	G_{12}	kPa	408,000	4,080,000	40,800,000
	G_{13}	kPa	400,000	4,000,000	40,000,000
	G_{23}	kPa	1,330,000	13,300,000	133,000,000
Poisson's ratio	ν	-	0	0	0
Element thickness	d	m	0.42	0.42	0.42

Table 3.4: Struts Parameters for Plane Strain Analysis

Identification	**EA** (kN)	**|Fmax,comp|** (kN)	**|Fmax,tens|** (kN)	**L spacing** (m)
Strut	4551000	1.10^{15}	1.10^{15}	5.00

Table 3.5: Waler and Struts Parameters for Three-dimensional Analysis

Parameter	**Name**	**Primary Strut**	**Secondary Strut**	**Waler**	**Unit**
Type of behavior	Type	Linear	Linear	Linear	-

Cross section area	A	0.0222	0.0307	0.008682	m^2
Volumetric weight	γ	78.5	78.5	78.5	kN/m^3
Young's modulus	E	$2.05.10^8$	$2.05.10^8$	$2.1.10^8$	kN/m^2
Moment of inertia	I_3	$5.4.10^{-4}$	$9.14.10^{-4}$	$1.045.10^{-4}$	m^4
	I_2	$5.4.10^{-4}$	$9.14.10^{-4}$	$3.668.10^{-4}$	m^4
	I_{23}	0.0	0.0	0.0	m^4

3.4.3 Excavation Stages

The excavation sequence consists of 17 stages for plane strain analysis, and 22 stages for three-dimensional analysis. The additional five stages in three-dimensional analysis are due to installation of secondary struts. The excavation stages for both plane strain and three-dimensional analyses are tabulated in *Table 3.6* below.

Table 3.6: Excavation Stages for Plane Strain and Three-dimensional Analyses

Stage for		**Action**
2D	**3D**	
1	1	Activate the wall
2	2	Deactivate the soil between 0 to 2 m depth, reset displacement to 0
3	3	Deactivate the soil between 2 to 3 m depth
4	4	Activate topmost primary struts; for 3D, activate waler too
-	5	Activate topmost secondary struts and waler
5	6	Deactivate the soil between 3 to 5 m depth
6	7	Deactivate the soil between 5 to 6 m depth
7	8	Activate the second topmost primary struts; for 3D, activate waler too
-	9	Activate the second topmost secondary struts and waler
8	10	Deactivate the soil between 6 to 8 m depth
9	11	Deactivate the soil between 8 to 9 m depth
10	12	Activate the middle primary struts; for 3D, activate waler too
-	13	Activate the middle secondary struts and waler

11	14	Deactivate the soil between 9 to 11 m depth
12	15	Deactivate the soil between 11 to 12 m depth
13	16	Activate the second lowest primary struts; for 3D, activate waler too
-	17	Activate the second lowest secondary struts and waler
14	18	Deactivate the soil between 12 to 14 m depth
15	19	Deactivate the soil between 14 to 15 m depth
16	20	Activate the lowest primary struts; for 3D, activate waler too
-	21	Activate the lowest secondary struts and waler
17	22	Deactivate the soil between 15 to 16 m depth

3.4.4 Plaxis Models for the Parametric Study

Using symmetry boundary conditions along the lines of symmetry, only half of the problem is considered in plane strain analyses. In three-dimensional analyses, only a quarter of the model is considered.

Plane strain analyses using Plaxis 2D utilizes 15-node triangular elements to define soil layers. The 15-node triangle provides fourth order interpolation for displacement and twelve Gauss points (stress points) for numerical integration. This element mode is chosen for greater accuracy for difficult problems.

For three-dimensional analysis using Plaxis 3D, 15-node wedge elements are used. This type of element provides second order interpolation of displacements and six Gauss points for integration.

Both plane strain and three-dimensional models were modeled with coarse global coarseness. However local refinement is applied in the wall plate for the plane strain models, and in the excavation cluster for the three-dimensional models.

For the three-dimensional analyses, the excavation length (L) is varied from 20 m to 60 m in the three cases, such that L/H_e varied from 1.25 to 3.75 and L/B is varied from 1 to 3. For all cases, 'roller' fixities are added to the boundaries to restrain horizontal displacement in

perpendicular direction to the boundary, and to restrain horizontal and vertical displacements at the bottom boundary. Roboski (2004) recommended the minimum distance of $5H_e$ from the mesh boundaries to the excavation boundaries. In all cases, the mesh boundaries are located at 120 m from the excavation boundaries, which is $7.5H_e$. The installation of the wall is assumed to induce no displacements to the adjacent soil, ie. the displacement is set to be zero after activation of the wall. Soil is excavated uniformly 1 m below primary strut level prior to installing the strut.

Figures 3.7 and *Figure 3.8* show the typical geometry and mesh of plane strain and three-dimensional models, while *Figures 3.9* and *3.10* show the typical deformed mesh of these models.

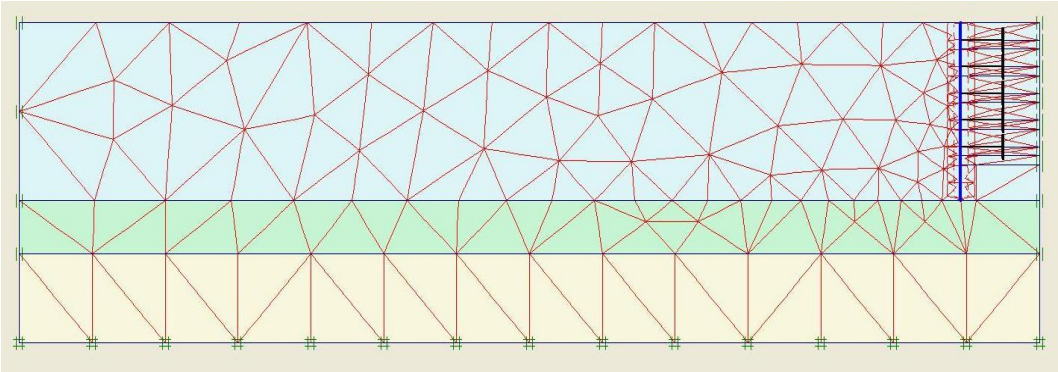

Figure 3.7: Typical Mesh of Plane Strain Model

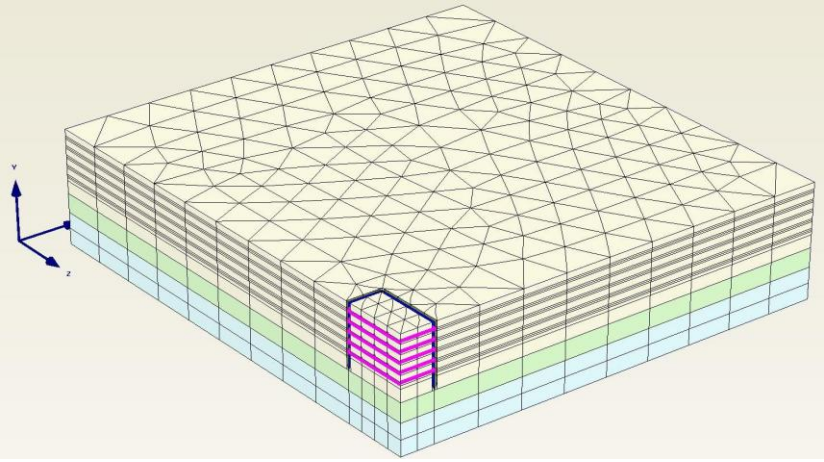

Figure 3.8: Typical Three-dimensional Mesh of Three-dimensional Model

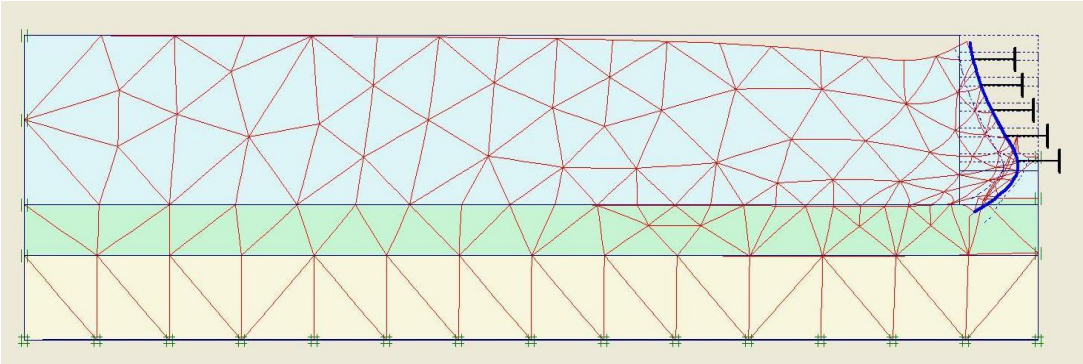

Figure 3.9: Typical Deformed Mesh of Plane Strain Model

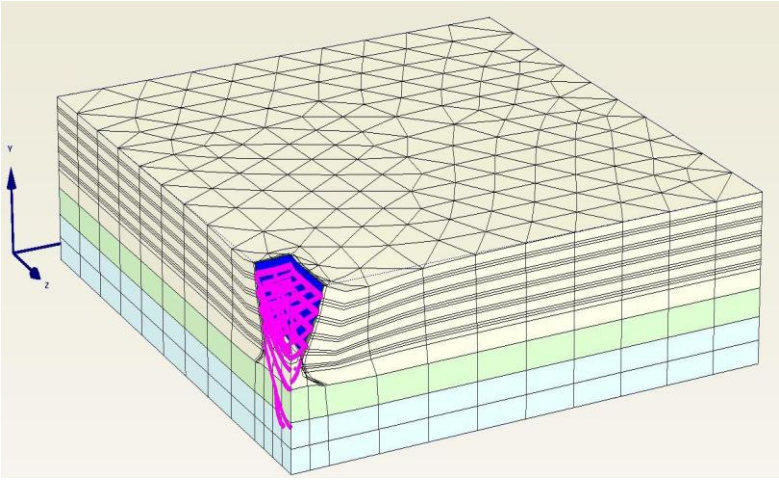

Figure 3.10: Typical Deformed Mesh of Three-dimensional Model

CHAPTER 4
RESULTS AND ANALYSES

The results of the analyses are represented by cases comparison and plane strain ratio (PSR). Following Finno (2007), PSR is defined as the ratio of maximum movement in the center of an excavation wall obtained from three-dimensional analyses to the maximum movement obtained from plane strain analyses.

The results of maximum lateral movements and bending moments are with reference to the end of the construction phases. The results of strut forces represent maximum strut forces experienced by the primary struts regardless of the phases.

4.1 Lateral Movements of the Primary Wall – General Trends

In general, the pattern of lateral wall movements into the excavation area of the primary wall from plane strain and three-dimensional analyses are illustrated in *Figure 4.1*. The results presented in these figures reflect the effect of wall stiffness to lateral movements, in which stiffest walls (shown by cases C) have the smallest movement as compared to flexible or medium walls. The detailed results of lateral movements of the primary wall can be found in *Appendix B.*

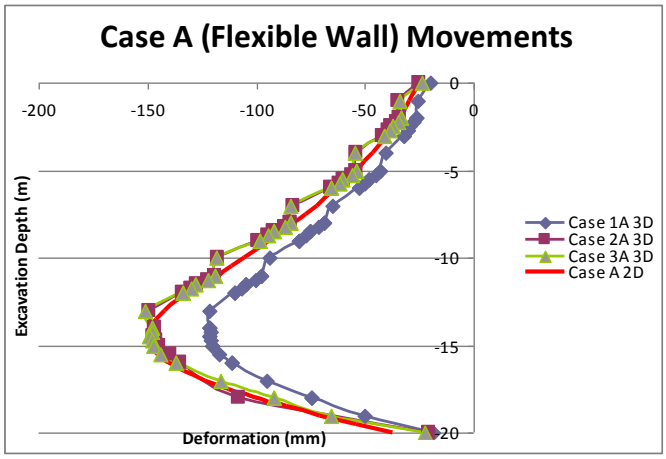

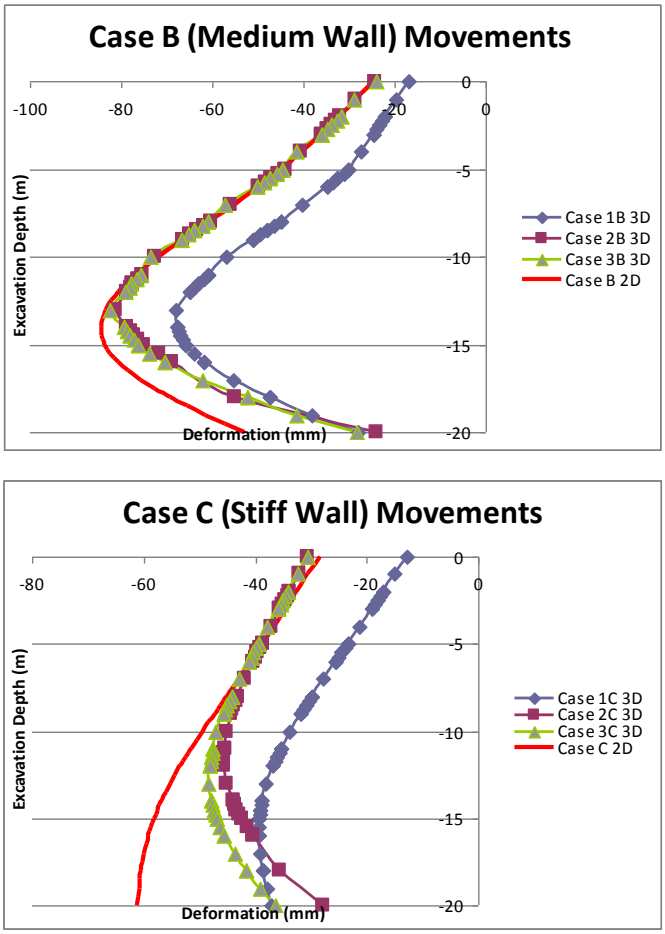

Figure 4.1: Lateral Movements of Primary Wall of Cases A, B and C

From *Figure 4.1* above, it can be seen that three-dimensional results show clearer distinctions in lateral movement profile between flexible, medium and stiff walls. Jagged lines are shown in lateral movement profiles for flexible walls, especially at levels where the struts are installed. The profiles are smooth and smoother for cases of medium and stiff walls.

In general, the maximum lateral wall movements occur slightly above the excavation base. *Figure 4.1* shows that plane strain analyses yield higher movements as compared to the three-dimensional analyses. Cases 2 and Cases 3 yield more similar results with plane strain analyses. On the other hand, Cases 1 yields noticeably smaller lateral movements.

This trend is also reflected by the maximum lateral wall movements profile as shown in the *Figure 4.2* and *Table 4.1* below. The negative sign merely shows the direction of wall movements with respect to x-axis on the model.

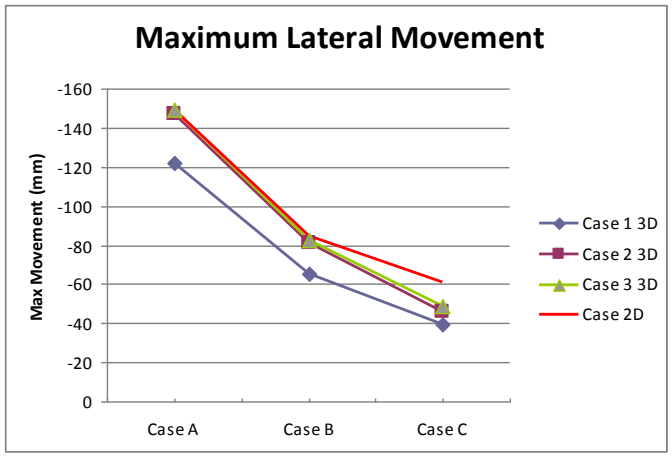

Figure 4.2: Maximum Lateral Movements of Primary Wall

Table 4.1: Maximum Lateral Movements of Primary Wall

Analysis	**Case**	δ_{max} **of Primary Wall (mm)**
2D	A	-149.14
	B	-84.44
	C	-61.14
3D	1A	-121.72
	1B	-64.95
	1C	-39.36
	2A	-147.14
	2B	-81.28
	2C	-45.60
	3A	-149.05
	3B	-82.36
	3C	-48.47

Even though the difference in excavation length between Cases 1, 2 and 3 is same, which is 20 m in length, the figures above clearly show that the result of lateral wall movements of Case 2 is really close to that of Case 3, as compared to Case 1 to Case 2. This indicates that the influence of the excavation length on the lateral movements is not linear.

4.1.1 Effects of Excavation Size

Effect of excavation size to the lateral wall movements can be evaluated using plane strain ratio (PSR), by comparing the PSR value of cases with different excavation length. L/H_e ratio is 1.25, 2.5 and 3.75, and L/B ratio is 1, 2 and 3 for Cases 1, 2 and 3 respectively.

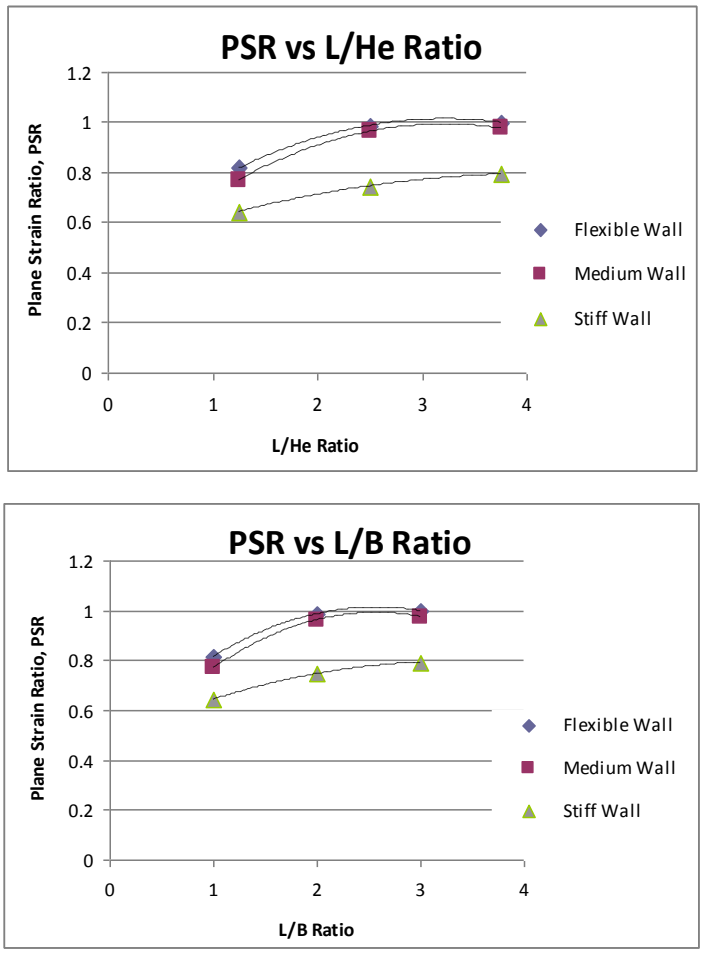

Figure 4.3: Effect of Excavation Size to PSR

Figure 4.3 shows that as L/H_e increases, the PSR value is closer to 1, which depicts the similarity in maximum primary wall movement in the center of the excavation of three-dimensional to plane strain analyses. As L/H_e decreases, the PSR ratio decreases, regardless of the stiffness of the wall. Understandably, as B is constant while L varies, similar result can be observed from L/B ratio.

For flexible and medium walls, PSR equals to 1 is reached when the L/H_e ratio is greater than 3 and when L/B ratio is greater than 2.5. This result indicates that L/H_e ratio is more critical than L/B ratio.

In general, the PSR result supports the argument that the corner stiffening effect diminishes as the excavation area is larger, and consequently, more apparent when the excavation length is smaller.

4.1.2 Effects of Wall Stiffness

In flexible and medium walls, PSR equals to 1 is reached when L/H_e ratio is greater than 3 and when L/B ratio is greater than 2.5. However for the case of stiff wall, the PSR value remains low, which suggests that stiff wall has more restraining effect as compared to the more flexible walls.

This restraining effect is provided by the stiff secondary wall which reduces the corner movements, and consequently reduces the movements of the primary wall.

Due to time constraint, further studies on cases with larger L/H_e and L/B ratios are not conducted. This study therefore suggests that to investigate wall movements, three-dimensional analyses are recommended for stiff wall. However, for flexible and medium walls, plane strain analyses are sufficient when L/H_e ratio is greater 3 and when L/B ratio is greater than 2.5, provided that H_e and B are constant.

4.2 Bending Moments of the Primary Wall

The trends of bending moments of primary wall from plane strain and three-dimensional analyses are shown in *Figure 4.4*. The positive and negative signs of the bending moment values merely show the direction of bending with respect to x-axis. Maximum bending moment occurs near the level of maximum deformation, or slightly above the excavation base. The flexible wall yields smallest bending moment, while the stiff wall yields largest bending moment.

The more flexible the wall, the lesser resistance to the forces exerted onto the wall by primary struts, hence the jagged bending moment profiles on primary strut levels.

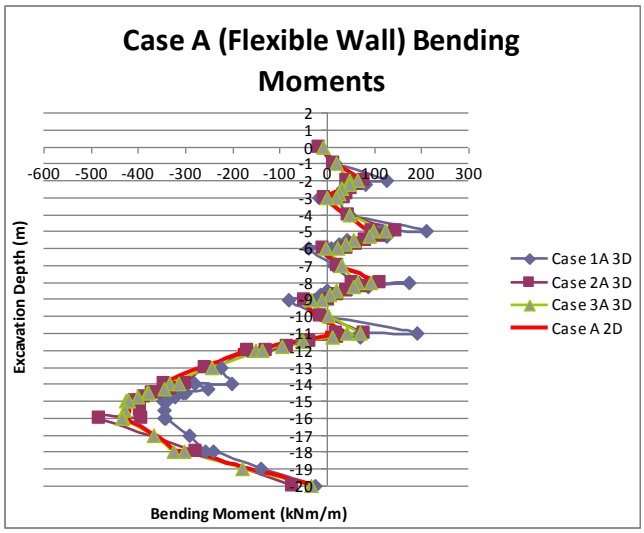

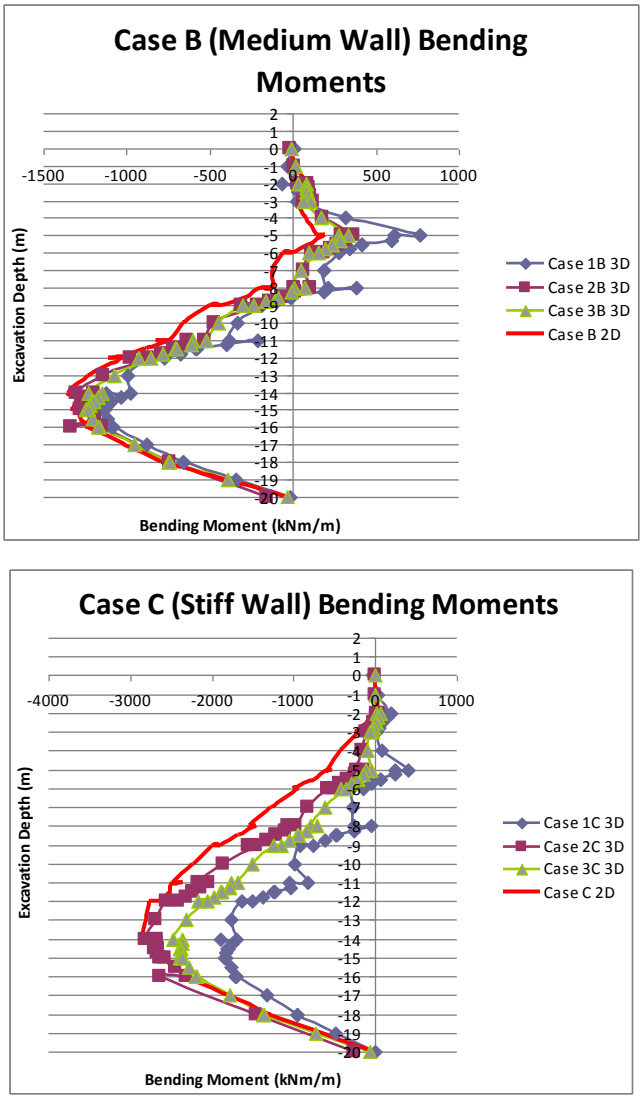

Figure 4.4: Wall Bending Moments of Cases A, B and C

The trend of maximum bending moment is reflected by comparison of the maximum bending moments as shown in the *Figure 4.5*. Consistent with the trend of wall movement discussed in the previous section, the maximum bending moment comparison shown in *Figure 4.5* below shows that Case 2 and Case 3 maximum bending moments are closer to that of plane strain analysis as compared to Case 1.

The detailed results of bending moments of primary wall are presented in *Appendix C*.

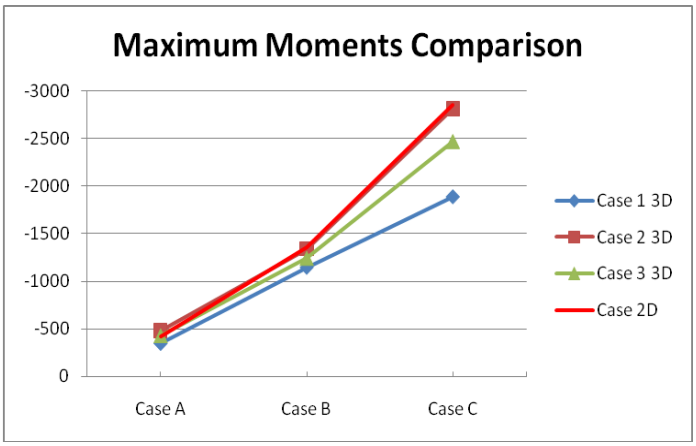

Figure 4.5: Maximum Wall Bending Moments of Cases A, B and C

4.3 Lateral Earth Pressure

The lateral earth pressures for all cases in general follow the trend shown by *Figure 4.6* below. For the earth pressure diagrams of all cases and detailed results of lateral earth pressure for plane strain and three-dimensional cases, refer to *Appendix D.*

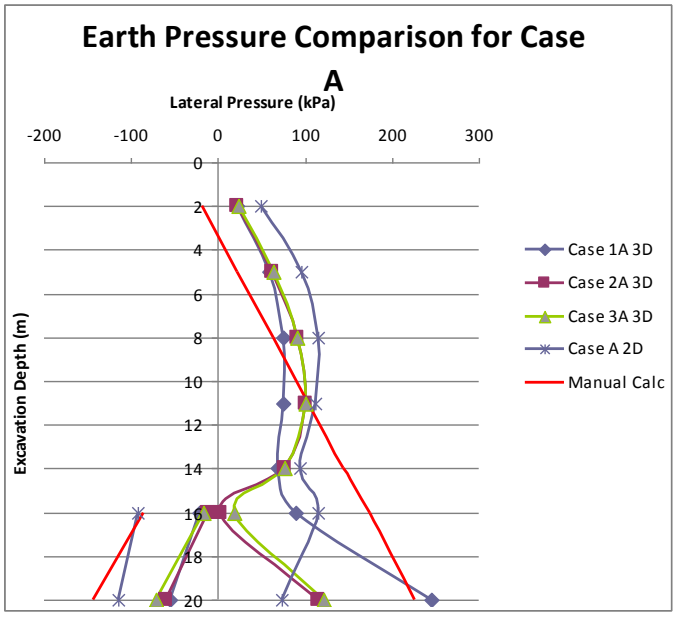

Figure 4.6: Lateral Earth Pressure Diagram for Cases of Flexible Wall

The red lines represent active and passive lateral earth pressures based on Rankine's theory.

The lateral earth pressures seem to correlate with the lateral wall movements. In the cases of flexible wall, as shown by the *Figure 4.6*, the mode of wall movements is translational. Translational movement means that the wall body moves parallel to the same distance, without any rotation with respect to the top or bottom of the wall. The upper part of the excavation never reaches the active Rankine's line, due to the fact that the elements at the upper part of the backfill never failed in this mode of movement. As the lateral wall movements reach their maximum near the bottom of excavation, the active earth pressure decreases.

On the other side of the wall, the passive pressure has not been fully developed to the Rankine's passive state. However there is a considerable difference between passive pressure of plane strain model and those of three-dimensional models. This is related to the higher lateral wall movements below the excavation base from the plane strain model. The high lateral movements into the soil below the excavation base push the soil body inward, and consequently result in high passive pressure.

4.4 Strut Loads and Apparent Pressure Diagram

Plaxis analysis provides information of strut forces in every stage of excavation. However to compare the forces on the struts with Terzaghi-Peck's Apparent Pressure Diagrams (APD), only maximum strut forces, regardless of the stage of excavation, are considered.

The information of strut forces (in kN) are important to determine the equivalent horizontal pressure (in kPa). The maximum pressure on each strut is calculated by dividing the maximum strut forces to area extending horizontally at half the distance to the next vertical row of struts on each side, and vertically half the distance to the horizontal sets of struts immediately above and below. Detailed calculations and results are included in *Appendix E*.

The pressure diagrams from plane strain and three-dimensional analyses are shown in *Figure 4.7*. All struts are in compression.

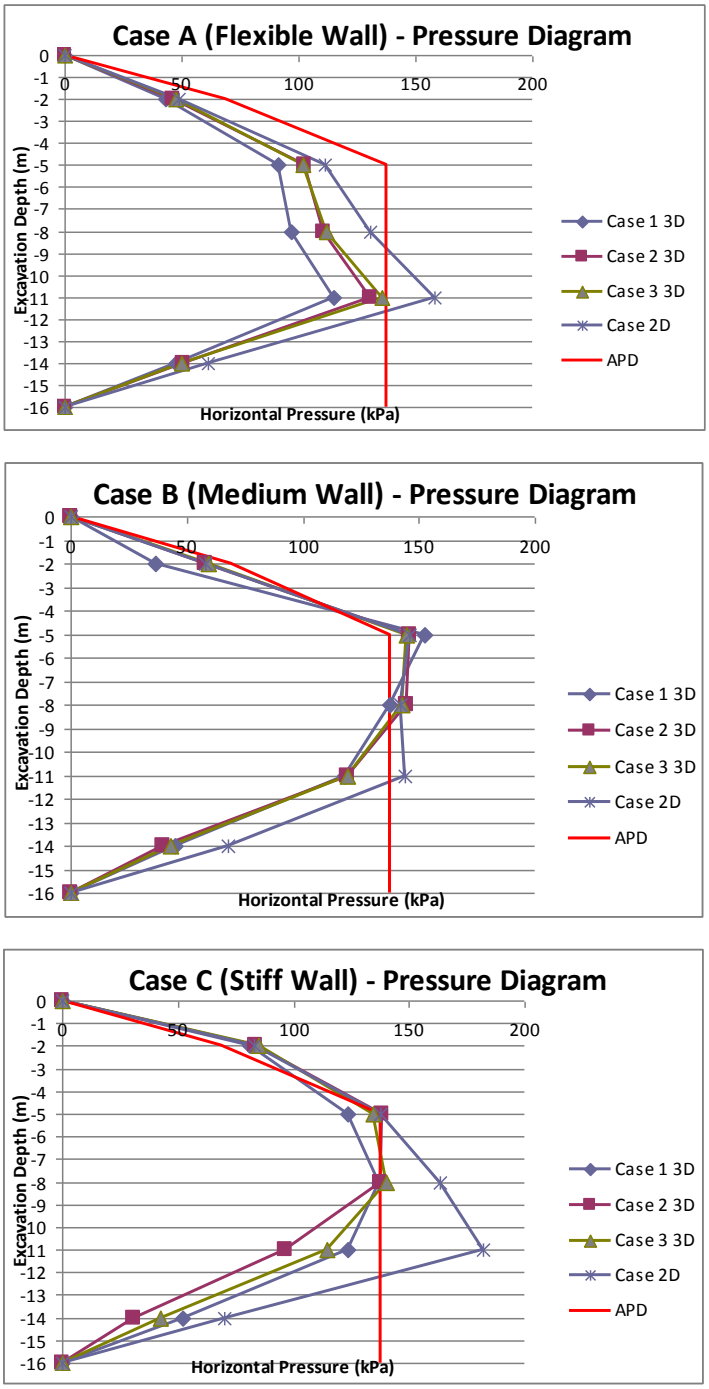

Figure 4.7: Comparison between Pressure Diagrams from Plaxis Analyses and from Terzaghi-Peck's APD

In general, higher strut loads can be expected for stiffer walls. The effect of stiffness is linked to the arching effect induced by wall movements, especially for flexible walls. The redistribution

of earth pressure corresponding to the arching effect on flexible wall results in lower bending moments. Greater flexibility of the wall results in greater moment reduction, which will also result in smaller strut load.

Even though the effect of wall stiffness is more significant, excavation geometry also affects the strut load. From *Figure 4.7* it can be seen that in general, struts from larger excavation area experience higher loads. This is probably due to the influence of corner effect in wall movements. As the length of excavation increases, the corner stiffening effect reduces, and therefore lateral wall movements increase. This causes the wall to deflect further into the excavation area and results in higher loads on the struts.

Figure 4.7 shows that Terzaghi and Peck's APD underestimate the strut loads of middle struts, and overestimate the strut loads of the lowest strut. These results agree with Chang and Wong (1996) on APD.

4.5 Lateral Movements of the Secondary Wall

In plane strain analyses, the effect of excavation on the movements of secondary wall cannot be studied. This study is only possible using three-dimensional analysis.

The lateral movements of the secondary wall in general agree with the results of the primary wall. Maximum lateral movement occurs slightly above the bottom of the excavation base. Flexible wall yields highest lateral movement as compared to medium and stiff walls.

Figure 4.8 shows that secondary wall movements are also dependent to the excavation geometry. As the length of excavation increases from Case 1 to Case 3, the secondary wall movements increase. This trend is also linked to the corner stiffening effect. With larger excavation area, the corner stiffening effect diminishes. As the result, lateral movements in primary wall increase. The increase in lateral movements also takes place at the corner of excavation. As the corner of the wall deflects, the corner stiffening effect onto the secondary wall decreases, and therefore causes the secondary wall to deform more.

Detailed results of lateral wall movements of secondary wall are presented in *Appendix F*.

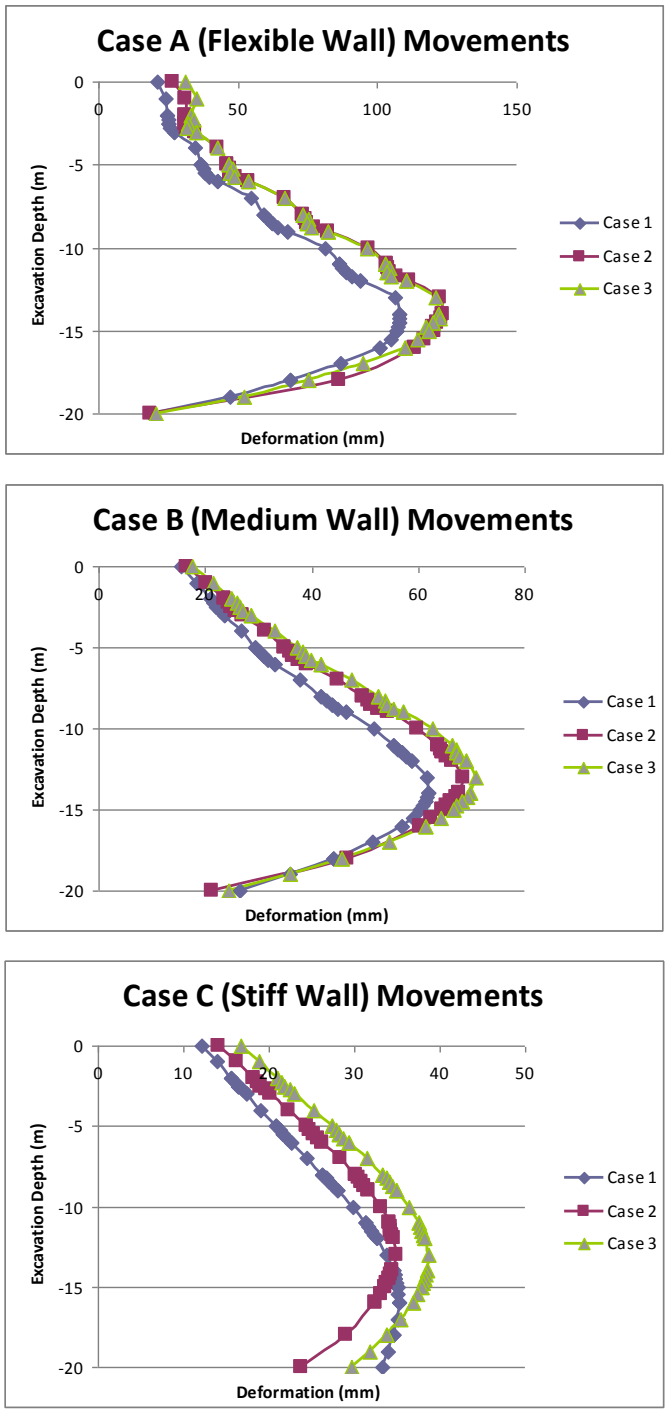

Figure 4.8: Lateral Movements of Secondary Wall of Cases A, B and C

4.6 Strut Failure Condition

In one strut failure analysis, the lowest strut is assumed to have failed. Therefore in all the analyses, the lowest strut is removed. Only three aspects from strut failure condition will be discussed here, namely the lateral wall movements, lateral earth pressure, and distribution of strut forces.

4.6.1 Lateral Movements of the Primary Wall after Failure

As strut failure occurs on the lowest strut level, the maximum lateral movement of the primary wall increases. The trend of maximum lateral movement of the primary wall before strut failure has been previously presented on *Figure 4.3* and *Table 4.1*. *Table 4.2* below presents the comparison of maximum primary walls movement before and after failure, so as to illustrate the effect of lowest strut failure on braced excavation. The detailed results of lateral movements of primary wall after strut failure condition are presented in *Appendix G*.

Table 4.2 Maximum Lateral Movements of Primary Wall: Before and After Strut Failure

Analysis	**Case**	δ_{max} **Before Failure (mm)**	δ_{max} **After Failure (mm)**
2D	A	-149.14	-173.78
	B	-84.44	-116.53
	C	-61.14	-94.56
3D	1A	-121.72	-128.87
	1B	-64.95	-71.73
	1C	-39.36	-40.47
	2A	-147.14	-154.43
	2B	-81.28	-82.88
	2C	-45.60	-45.92
	3A	-149.05	-156.31
	3B	-82.36	-84.09
	3C	-48.47	-49.11

As can be seen from *Table 4.2*, the lateral movements of the primary wall increase. The increase is more significant for the plane strain analysis. The increase in wall movements ranges from 15% to 36%. In three-dimensional analysis, the increase in wall movements is smaller, with the maximum increase being only 9.5%. This is probably due to the installation of walers in the three-dimensional models. In plane strain analysis, the walers cannot be modeled. From the comparison table above, the installation of walers is shown to increase the stiffness of the wall, and prevents significant increase in lateral wall movements.

4.6.2 Lateral Earth Pressure after Failure

The lateral earth pressures after the lowest strut failure for all cases in general follow the trend shown by *Figure 4.9* below.

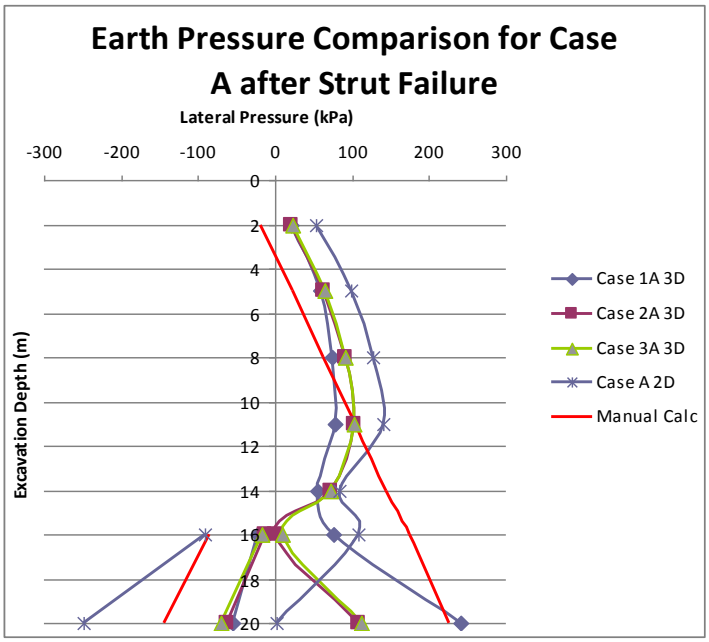

Figure 4.9: Earth Pressure Diagram for Cases of Flexible Wall after Strut Failure

After lowest strut failure, the passive pressures from plane strain model noticeably increase and exceed the Rankine's passive pressure. This is related to the lateral wall movements after strut failure. Compared to three-dimensional models, plane strain models yield higher additional wall movements at the lower level of excavation and below the excavation base, thus result in higher

passive pressures to the soil. For the detailed results of lateral earth pressure after strut failure, please refer to *Appendix H.*

4.6.3 Distribution of Strut Forces

In plane strain analysis, forces that were previously carried by the failed strut are assumed to be distributed to the struts immediately above it for the lowest strut. However in three-dimensional analysis, this assumption is not entirely true, since these forces will also be distributed to other adjacent struts and support system. *Figure 4.10* shows the elevation view of struts arrangement as part of primary wall. The black rectangle represents the location of failed strut, and the rest of rectangles represent the adjacent struts.

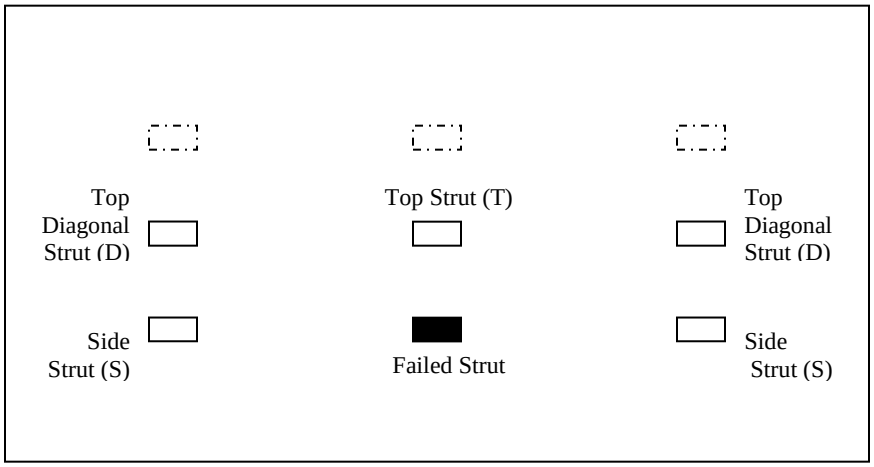

Figure 4.10: Elevation View of Struts Arrangement in Primary Wall

For this study, only strut forces distributed to the immediate adjacent struts are considered.

Figure 4.11 shows the percentages of force that are distributed to the adjacent struts in the case of lowest strut failure with respect to excavation area, obtained from three-dimensional analyses. Detailed calculations are presented in *Appendix I.*

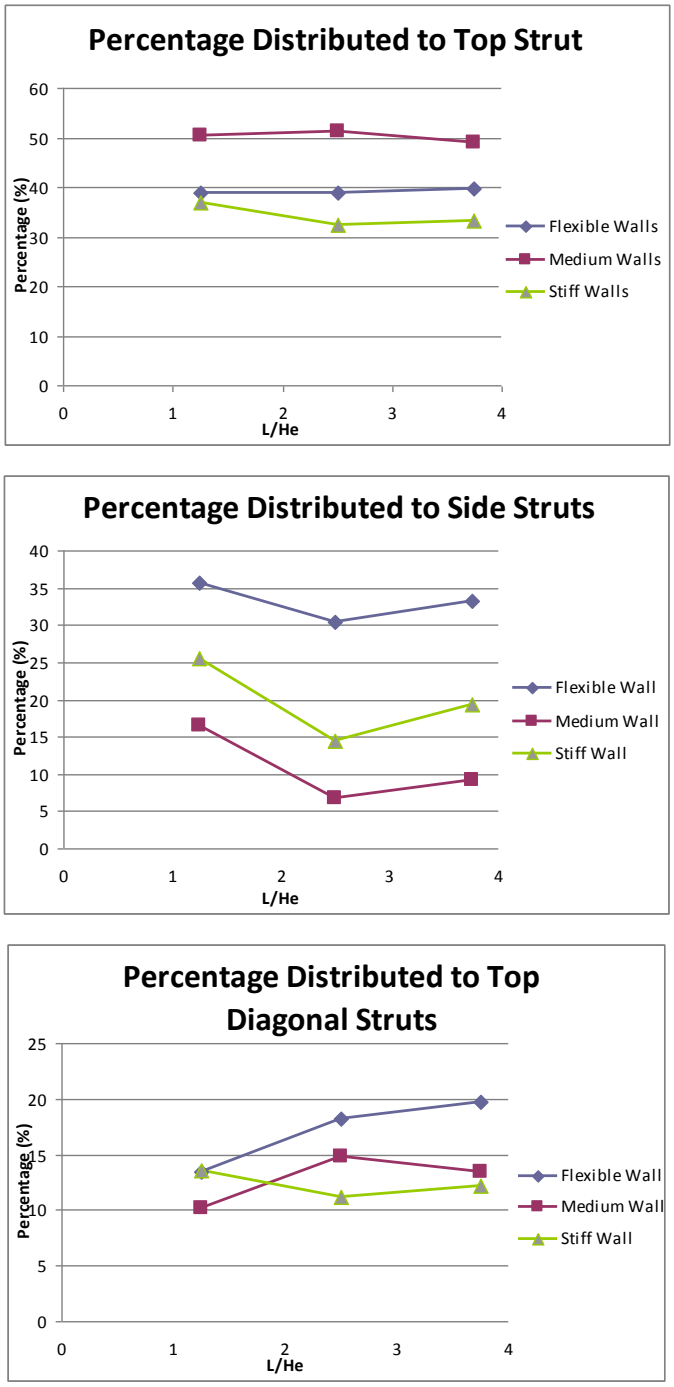

Figure 4.11: Percentage of Strut Forces Distributed to Adjacent Struts after Strut Failure

Figure 4.11 above shows that large portion of the forces, or 32 % to 52 % of the forces, are transferred to the strut immediately above the failed strut. The other majority portions of the

forces are distributed to struts on both right and left sides (6% to 36%), and struts on top both right and left diagonal of the failed strut (10% to 20%).

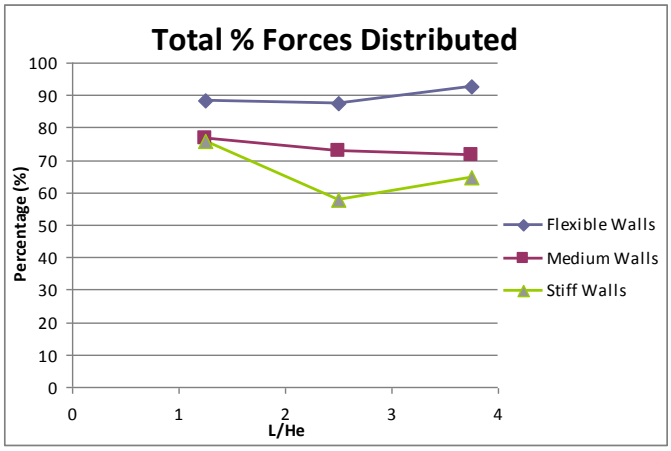

Figure 4.12: Total Percentage of Strut Forces Distributed to the Immediate Adjacent Struts after Lowest Strut Failure

The detailed figures of percentages of the distributed strut forces are tabulated in *Table 4.3* below. In this table, T refers to the strut immediately above, D refers to the strut immediately on the top left and right diagonal, and S refers to the strut immediately on the left and right side of the failed strut.

Table 4.3: Percentages of Strut Forces Distribution after Lowest Strut Failure

Case		**Flexible Walls (Case A)**			**Medium Walls (Case B)**			**Stiff Walls (Case C)**		
L/He		**1.25**	**2.5**	**3.75**	**1.25**	**2.5**	**3.75**	**1.25**	**2.5**	**3.75**
Strut (%)	**T**	39.01	38.80	39.64	50.30	51.22	48.96	36.93	32.34	33.22
	D	13.44	18.16	19.66	10.11	14.79	13.45	13.62	11.17	12.15
	S	35.73	30.35	33.19	16.48	6.68	9.13	25.51	14.37	19.40
	Total	88.17	87.31	92.49	76.89	72.69	71.54	76.06	57.89	64.77

Even though there is inconsistency in cases where L/H_e equals to 2.5, in general, the more flexible the wall is, the more forces are distributed to the adjacent struts, as can be observed from *Figure 4.12* and *Table 4.3*

Portions of forces which are not distributed to the immediate nearby struts are carried by the wall, waler and by the next adjacent struts. Stiffer walls will carry more forces as compared to more flexible walls.

CHAPTER 5
CONCLUSIONS AND RECOMMENDATIONS

5.1 Conclusions

The aim of this project is to examine the effect of corner stiffening effect to the performance of a braced excavation system using two-dimensional and three-dimensional geotechnical finite element programs. Twenty four cases of parametric study with various excavation length and wall stiffness are conducted, including cases of one strut failure condition.

The following conclusions can be drawn:

- Plane strain analyses yield more conservative results for lateral wall movements, bending moments, strut loads, and strut forces distributions after strut failure condition.
- For flexible and medium walls, plane strain simulations are sufficient for lateral wall movement analyses when L/H_e ratio is greater than 3 and L/B ratio is greater than 2.5, provided that H_e and B are constant. However, for the cases of stiff wall, three-dimensional analyses are recommended.
- The PSR depends on the geometry of the excavation, expressed as L/H_e ratio, L/B ratio and wall system stiffness. The higher the L/H_e and L/B ratios, the larger are the maximum lateral movements behind primary wall. The lower the wall stiffness, the larger are the maximum lateral primary wall movements.
- The lateral movements of secondary wall also depend on the excavation area, ie. the length of primary wall. As excavation length increases, the lateral wall movements of secondary wall increase.
- Three-dimensional analyses show that after lowest strut failure, only 32% to 52% of the strut forces are distributed to the strut immediately above the failed strut, as opposed to the plane strain analyses which assume all strut forces are distributed to top strut. The rest of the strut forces are carried by the wall, waler and other adjacent struts.
- The stiffer the wall, the lesser portion of forces is distributed to the surrounding struts.

5.2 Recommendations

From the parametric study for this project, it has been found that the plane strain simulation for wall movement analysis is sufficient for excavation with L/H_e ratio larger than 3 and L/B ratio larger than 2.5 for flexible and medium walls, provided that H_e and B are constant. However, the conclusion can not be clearly drawn for the case of stiff wall due to limited cases conducted.

More parametric studies can be conducted by including more varied excavation length, width and depth. The purpose is to obtain a better picture on the effect of excavation geometry to the corner stiffening effect, and also to generate more comprehensive guidelines whether or not an excavation can be sufficiently modeled using plane strain simulation.

In addition, another aspect of braced excavation system, such as basal heave stability can also be further investigated.

REFERENCES

Bono, N. A, Liu, T. K., and Soydemir, C., 1992. Performance of an internally braced slurry-diaphragm wall for excavation support. *Slurry walls: Design, Construction and Quality Control,* ASTM STP, Vol. 1129, pp. 347-360.

Brinkgreve R. B. J., 2007. *Plaxis 3D Foundation Material Models Manual Version 2,* A.A. Balkema, Netherlands.

Brinkgreve R. B. J., 2007. *Plaxis 3D Foundation Reference Manual Version 2,* A.A. Balkema, Netherlands.

Chang, J. D. and Wong, K. S., 1996. Apparent pressure diagram for braced excavations in soft clay with diaphragm wall. *Proceedings from International Symposium on Geotechnical Aspects of Underground Construction in Soft Ground*, London, pp. 87-92.

Clough, G. W. and Davidson, R. R., 1977. Effects of construction on geotechnical performance. *Stanford University Civil Engineering Research Report*, 1977, pp. 1-39.

Clough, G. W., Smith, E. M., and Sweeney, B.P., 1989. Movement control of excavation support system in soft clay. *Journal of Performance of Constructed Facilities,* Foundation Engineering Congress, Vol. 2, ASCE, Reston, Va., pp. 869-836.

Craig, R.F., 2004. *Craig's soil mechanics 7th edition.* Spon Press, New York.

Das, Braja., 2006. *Principles of geotechnical engineering, 6th edition.* Thomson, California.

Duncan, J. M. and Buchigiani, A. L., 1976. An engineering manual for settlement studies. *Geotechnical Engineering Report*, Department of Civil Engineering, University of California, Berkeley, p. 94.

ETH Zurich, 2004. *Modeling in Geotechnics*. Institute of Geotechnical Engineering. http://geotech4.ethz.ch/mig

Finno, R. J., Blackburn, J. T., and Roboski, J.F., 2007. Three-dimensional effects for supported excavations in clay. *Journal of Geotechnical and Geoenvironmental*, Vol. 133, No. 1, pp. 30-36.

Halim, D., 2008. Effect of excavation on performance of adjacent buildings. *Ph.D. Thesis*, Nanyang Technological University, Singapore.

Lee, F.H., Yong, K.Y., Quan, K.C.N., and Chee, K.T., 1998. Effect of corners in strutted excavation: Field monitoring and case histories. *Journal of Geotechnical and Geoenvironmental*, Vol. 124, No. 4, 339-349.

Mana, A. I., and Clough, G. W., 1981. Prediction of movement for braced cuts in clay. *Journal of Geotechnical Engineering Division*, ASCE, Vol. 107, No. GT6, pp. 759-777.

Ou, C.Y., Chiou, D.C., and Wu, T.S., 1996. Three dimensional finite element analysis of deep excavations. *Journal of Geotechnical Engineering*, Vol. 122, No. 5, pp. 337-345.

Peck, R. B., 1969. Deep excavations and tunneling in soft ground. *Proceedings from 7th International Conference on Soil Mechanics and Foundation Engineering*, Mexico City, State of the Art Volume, pp 225-290.

Potts, D.M., and Zdravkovic L., 1999. *Finite element analysis in geotechnical engineering: Theory*. Thomas Telford, London.

Roboski, J. F., 2004. Three-dimensional performance and analysis of deep excavations. *Ph.D. Thesis*, Northwestern Univ., Evanston, Illinois.

Stroud, M. A., 1974. The standard penetration test in insensitive clays and soft rocks. *Proceedings from European Conference on Penetration Test*, Vol. 2, No. 2, pp. 367-375.

Terzaghi, K. and Peck, P.B., 1967. *Soil mechanics in engineering practice, 2nd edition*, John Wiley & Sons, New York.

Wong, K. S. and Broms, B. B., 1989. Lateral wall deflections of braced excavation in clay. *Journal of Geotechnical Engineering Division*, ASCE, Vol. 115, No. 6, pp. 853-870.

Wong, K.S., 2003. Observational approach to avoid failures in temporary works. *Seminar on Avoiding Failures in Excavation Works,* Building & Construction Authority, Singapore, 11 July 2003.

Wong, K.S., 2004. How to avoid failures in deep excavation. *Proceedings of International Conference on Structural and Foundation Failures,* Singapore, pp. 384-397.

Appendix A: Finite Element Methods

Finite element analysis involves division of a domain into many smaller parts. Approximation of solution for each part is obtained from linear combination of nodal values and approximation functions. The solution from each part is then assembled to obtain the solution of whole domain. The division of domain has advantages as it allows accurate representation of solution with each element to bring out local effects.

Since the shear strength of a soil at given point depends on the effective stress at that point, the stress strain response of a soil is highly non-linear. Therefore the geotechnical finite element program should have the following features:

- Material models which are capable of modeling non-linear stress-strain behavior which include options for undrained analysis (short-term behavior), drained analysis (long-term behavior) and coupled consolidation analysis.
- The ability to specify non-zero in-situ stresses.
- The ability to add or remove elements during the analysis, especially for modeling constructions or excavations.

A.1 Element Discretisation

The modeling of problem under investigation requires assemblage of whole geometry, or domain, into small regions called finite element. These finite elements will form finite element mesh which will replace the geometry of problem under investigation. Most finite elements for plane strain analysis are triangular or quadrilateral in shape; while for three-dimensional analysis, the popular elements are tetrahedral and hexahedral as shown in *Figure 3.1*.

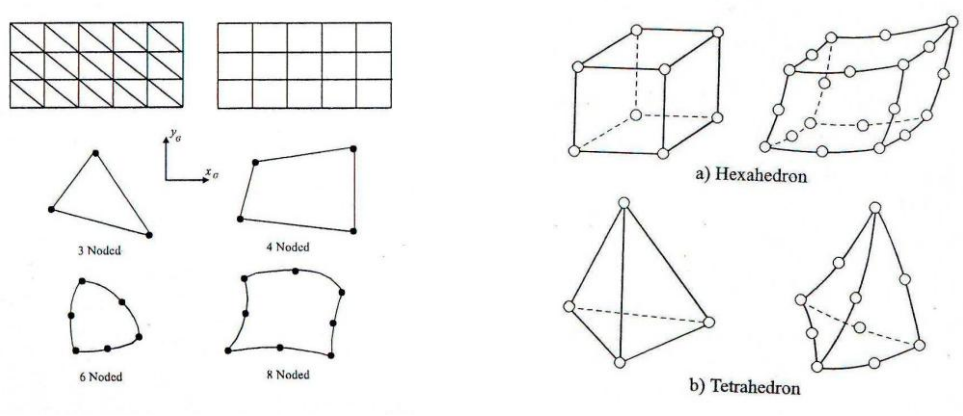

Figure A.1: On the Left: Typical Finite Elements in Plane Strain Analysis. On the right: Typical Finite Elements in Three-Dimensional Analysis.

Geometry of finite elements is specified by nodes in corners, as well as along the element boundary, depending on element shape.

Unlike other materials, soil has no well-defined physical or mechanical properties. Soil properties vary from site to site and are influenced by many factors. Therefore careful selections of finite element model and mesh of elements which can sufficiently represent the problem and its soil physical features must be ensured for a successful analysis.

A.2 Excavation in Geotechnical Finite Element Analysis

Simulation of excavation or unloading of soil in the finite element analysis can be summarized as follows. *Figure 3.2a* shows the soil body consists of portion A and B. Portion A is to be excavated, leaving portion B. Once the portion A is removed, no displacements or changes in stress occur. However, portion A is then replaced by tractions (T) whose values are equal to internal stresses in soil mass on the excavated surface before portion A is removed. This is shown in *Figure 3.2b*. The behavior of portion B can then be identified by removing the tractions (T), for example by applying equal and opposite tractions, as shown in *Figure 3.2c*.

This simulation involves determination of tractions (T) at the new soil boundary, stiffness of soil mass, and application of tractions –T to the new soil boundary.

In braced excavation simulation, structural elements such as walers, and struts are added as excavation progress. It is therefore necessary to split the analysis into sequence of increments, and to use nonlinear constitutive model.

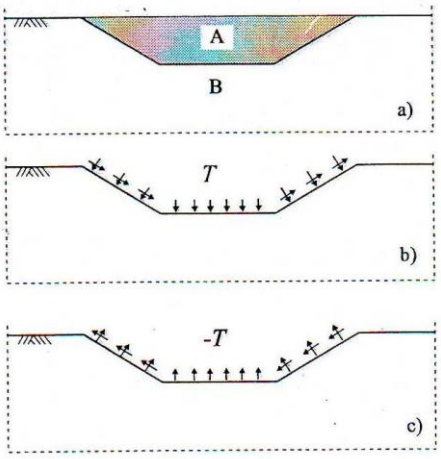

Figure A.2: Simulation of Excavation in Finite Element Analysis

Appendix B: Lateral Movements of the Primary Wall

B.1 Plane Strain Analysis

Table B.1: Lateral Wall Movements from Plane Strain Analysis

Case 1A		Case 1B		Case 1C	
Y	**Ux**	**Y**	**Ux**	**Y**	**Ux**
[m]	**[mm]**	**[m]**	**[mm]**	**[m]**	**[mm]**
0	-25.1118	0	-24.5717	0	-28.459
-0.5	-27.2577	-0.5	-26.4686	-0.5	-29.4666
-1	-29.4272	-1	-28.3678	-1	-30.4745
-1.5	-31.6925	-1.5	-30.2762	-1.5	-31.4829
-2	-34.171	-2	-32.2041	-2	-32.4928
-2	-34.171	-2	-32.2041	-2	-32.4928
-2.25	-35.5585	-2.25	-33.1803	-2.25	-32.9985
-2.5	-37.0157	-2.5	-34.1649	-2.5	-33.5049
-2.75	-38.5236	-2.75	-35.1583	-2.75	-34.0119
-3	-40.0673	-3	-36.1615	-3	-34.5198
-3	-40.0673	-3	-36.1615	-3	-34.5198
-3.5	-43.2281	-3.5	-38.2026	-3.5	-35.5382
-4	-46.4819	-4	-40.3038	-4	-36.5618
-4.5	-49.9037	-4.5	-42.4884	-4.5	-37.5926
-5	-53.6692	-5	-44.7887	-5	-38.6336
-5	-53.6692	-5	-44.7887	-5	-38.6336
-5.25	-55.8014	-5.25	-45.9997	-5.25	-39.1596
-5.5	-58.0443	-5.5	-47.2438	-5.5	-39.6885
-5.75	-60.3609	-5.75	-48.5156	-5.75	-40.2199
-6	-62.722	-6	-49.8105	-6	-40.7532
-6	-62.722	-6	-49.8105	-6	-40.7532

-6.5	-67.499	-6.5	-52.4543	-6.5	-41.8247
-7	-72.2962	-7	-55.1522	-7	-42.9009
-7.5	-77.1631	-7.5	-57.8935	-7.5	-43.9809
-8	-82.2817	-8	-60.6805	-8	-45.0654
-8	-82.2817	-8	-60.6805	-8	-45.0654
-8.25	-85.0701	-8.25	-62.1006	-8.25	-45.6104
-8.5	-87.9513	-8.5	-63.5259	-8.5	-46.1558
-8.75	-90.8864	-8.75	-64.9478	-8.75	-46.7005
-9	-93.8451	-9	-66.3582	-9	-47.2436
-9	-93.8451	-9	-66.3582	-9	-47.2436
-9.5	-99.7574	-9.5	-69.1173	-9.5	-48.3216
-10	-105.622	-10	-71.7577	-10	-49.384
-10.5	-111.511	-10.5	-74.2489	-10.5	-50.427
-11	-117.637	-11	-76.5755	-11	-51.4483
-11	-117.637	-11	-76.5755	-11	-51.4483
-11.25	-120.95	-11.25	-77.6819	-11.25	-51.9513
-11.5	-124.323	-11.5	-78.7351	-11.5	-52.4472
-11.75	-127.679	-11.75	-79.7241	-11.75	-52.9344
-12	-130.949	-12	-80.639	-12	-53.4118
-12	-130.949	-12	-80.639	-12	-53.4118
-12.5	-136.997	-12.5	-82.212	-12.5	-54.3322
-13	-142.069	-13	-83.3948	-13	-55.2002
-13.5	-145.883	-13.5	-84.1444	-13.5	-56.0099
-14	-148.266	-14	-84.4348	-14	-56.7573
-14	-148.266	-14	-84.4348	-14	-56.7573
-14.25	-148.915	-14.25	-84.4062	-14.25	-57.1074
-14.5	-149.143	-14.5	-84.2553	-14.5	-57.4409
-14.75	-148.913	-14.75	-83.9784	-14.75	-57.7575
-15	-148.193	-15	-83.5729	-15	-58.0569
-15	-148.193	-15	-83.5729	-15	-58.0569
-15.25	-146.962	-15.25	-83.0372	-15.25	-58.339

-15.5	-145.203	-15.5	-82.371	-15.5	-58.6039
-15.75	-142.909	-15.75	-81.5751	-15.75	-58.8517
-16	-140.081	-16	-80.6516	-16	-59.0828
-16	-140.081	-16	-80.6516	-16	-59.0828
-16.5	-132.869	-16.5	-78.4361	-16.5	-59.4971
-17	-123.688	-17	-75.7592	-17	-59.8516
-17.5	-112.675	-17.5	-72.6638	-17.5	-60.1526
-18	-100.002	-18	-69.2006	-18	-60.4074
-18	-100.002	-18	-69.2006	-18	-60.4074
-18.5	-85.8726	-18.5	-65.4282	-18.5	-60.6241
-19	-70.5302	-19	-61.4123	-19	-60.8114
-19.5	-54.291	-19.5	-57.2276	-19.5	-60.979
-20	-37.556	-20	-52.9559	-20	-61.1369

B.2 Three-dimensional Analysis

Table B.2: Lateral Wall Movements of Case 1 from Three-dimensional Analysis

Case 1A		**Case 1B**		**Case 1C**	
Y	**Ux**	**Y**	**Ux**	**Y**	**Ux**
[m]	**[mm]**	**[m]**	**[mm]**	**[m]**	**[mm]**
0	-19.6912	0	-16.9549	0	-12.8898
-1	-25.6164	-1	-19.8196	-1	-14.981
-2	-26.5461	-2	-22.1283	-2	-17.0352
-2	-26.5461	-2	-22.1283	-2	-17.0352
-2.25	-27.6718	-2.25	-22.7012	-2.25	-17.5625
-2.5	-29.5579	-2.5	-23.3498	-2.5	-18.0968
-2.5	-29.5579	-2.5	-23.3498	-2.5	-18.0968
-2.75	-30.5137	-2.75	-23.9295	-2.75	-18.6237
-3	-32.2307	-3	-24.5949	-3	-19.1564
-3	-32.2307	-3	-24.5949	-3	-19.1564
-4	-40.6789	-4	-27.4802	-4	-21.281

-5	-42.8654	-5	-30.1046	-5	-23.3448
-5	-42.8654	-5	-30.1046	-5	-23.3448
-5.25	-44.9314	-5.25	-31.1956	-5.25	-23.8939
-5.5	-48.0747	-5.5	-32.4674	-5.5	-24.4535
-5.5	-48.0747	-5.5	-32.4674	-5.5	-24.4535
-5.75	-49.8797	-5.75	-33.588	-5.75	-24.9979
-6	-52.5872	-6	-34.8532	-6	-25.55
-6	-52.5872	-6	-34.8532	-6	-25.55
-7	-65.0558	-7	-40.3018	-7	-27.7242
-8	-68.9134	-8	-44.9311	-8	-29.7303
-8	-68.9134	-8	-44.9311	-8	-29.7303
-8.25	-71.3718	-8.25	-46.4067	-8.25	-30.2556
-8.5	-75.0655	-8.5	-48.0448	-8.5	-30.7884
-8.5	-75.0655	-8.5	-48.0448	-8.5	-30.7884
-8.75	-77.2392	-8.75	-49.4562	-8.75	-31.2943
-9	-80.2835	-9	-50.9726	-9	-31.804
-9	-80.2835	-9	-50.9726	-9	-31.804
-10	-93.7012	-10	-56.869	-10	-33.7358
-11	-97.695	-11	-60.7824	-11	-35.3282
-11	-97.695	-11	-60.7824	-11	-35.3282
-11.25	-100.483	-11.25	-61.8857	-11.25	-35.7251
-11.5	-104.551	-11.5	-63.0933	-11.5	-36.1234
-11.5	-104.551	-11.5	-63.0933	-11.5	-36.1234
-11.75	-106.969	-11.75	-63.9999	-11.75	-36.4816
-12	-110.007	-12	-64.9525	-12	-36.8382
-12	-110.007	-12	-64.9525	-12	-36.8382
-13	-121.578	-13	-67.9359	-13	-38.0841
-14	-121.314	-14	-67.6014	-14	-38.8128
-14	-121.314	-14	-67.6014	-14	-38.8128
-14.25	-121.194	-14.25	-67.3027	-14.25	-38.9536
-14.5	-121.715	-14.5	-67.0412	-14.5	-39.0917

-14.5	-121.715	-14.5	-67.0412	-14.5	-39.0917
-14.75	-121.03	-14.75	-66.5144	-14.75	-39.1922
-15	-120.128	-15	-65.8686	-15	-39.2721
-15	-120.128	-15	-65.8686	-15	-39.2721
-15.5	-117.139	-15.5	-64.1375	-15.5	-39.3599
-16	-111.511	-16	-61.7732	-16	-39.3538
-16	-111.511	-16	-61.7732	-16	-39.3538
-17	-94.9063	-17	-55.4524	-17	-39.0965
-18	-74.474	-18	-47.4127	-18	-38.5549
-18	-74.474	-18	-47.4127	-18	-38.5549
-19	-50.4319	-19	-38.284	-19	-37.8387
-20	-18.7329	-20	-28.0311	-20	-37.0184

Table B.2: Lateral Wall Movements of Case 2 from Three-dimensional Analysis

Case 2A		**Case 2B**		**Case 2C**	
Y	**Ux**	**Y**	**Ux**	**Y**	**Ux**
[m]	**[mm]**	**[m]**	**[mm]**	**[m]**	**[mm]**
0	-25.295	0	-24.3098	0	-30.4889
-1	-34.6414	-1	-28.7605	-1	-32.1888
-2	-34.3231	-2	-31.9248	-2	-33.7977
-2	-34.3231	-2	-31.9248	-2	-33.7977
-2.25	-35.4901	-2.25	-32.7953	-2.25	-34.2287
-2.5	-38.0139	-2.5	-33.8855	-2.5	-34.6759
-2.5	-38.0139	-2.5	-33.8855	-2.5	-34.6759
-2.75	-39.2821	-2.75	-34.8635	-2.75	-35.0901
-3	-41.9822	-3	-36.0107	-3	-35.5182
-3	-41.9822	-3	-36.0107	-3	-35.5182
-4	-54.1142	-4	-40.7453	-4	-37.21
-5	-53.8763	-5	-44.1188	-5	-38.7147
-5	-53.8763	-5	-44.1188	-5	-38.7147
-5.25	-55.994	-5.25	-45.4199	-5.25	-39.1488

-5.5	-60.0204	-5.5	-47.0181	-5.5	-39.602
-5.5	-60.0204	-5.5	-47.0181	-5.5	-39.602
-5.75	-62.0425	-5.75	-48.2559	-5.75	-39.9873
-6	-65.8745	-6	-49.7542	-6	-40.3915
-6	-65.8745	-6	-49.7542	-6	-40.3915
-7	-83.1887	-7	-56.1074	-7	-41.9404
-8	-84.3823	-8	-60.2378	-8	-43.0944
-8	-84.3823	-8	-60.2378	-8	-43.0944
-8.25	-86.9841	-8.25	-61.7145	-8.25	-43.4202
-8.5	-91.8074	-8.5	-63.517	-8.5	-43.7628
-8.5	-91.8074	-8.5	-63.517	-8.5	-43.7628
-8.75	-94.4755	-8.75	-64.8387	-8.75	-44.0158
-9	-98.9303	-9	-66.4198	-9	-44.2853
-9	-98.9303	-9	-66.4198	-9	-44.2853
-10	-117.556	-10	-72.6678	-10	-45.211
-11	-119.177	-11	-75.3618	-11	-45.4668
-11	-119.177	-11	-75.3618	-11	-45.4668
-11.25	-122.268	-11.25	-76.2485	-11.25	-45.5201
-11.5	-127.507	-11.5	-77.4068	-11.5	-45.5859
-11.5	-127.507	-11.5	-77.4068	-11.5	-45.5859
-11.75	-130.088	-11.75	-77.9673	-11.75	-45.5516
-12	-134.009	-12	-78.7434	-12	-45.531
-12	-134.009	-12	-78.7434	-12	-45.531
-13	-149.337	-13	-81.2781	-13	-45.2295
-14	-146.748	-14	-78.6933	-14	-44.004
-14	-146.748	-14	-78.6933	-14	-44.004
-14.25	-146.38	-14.25	-77.8837	-14.25	-43.6409
-14.5	-147.139	-14.5	-77.254	-14.5	-43.2875
-14.5	-147.139	-14.5	-77.254	-14.5	-43.2875
-14.75	-145.879	-14.75	-76.1641	-14.75	-42.8593
-15	-144.99	-15	-75.0318	-15	-42.4099

-15	-144.99	-15	-75.0318	-15	-42.4099
-15.5	-139.759	-15.5	-71.7377	-15.5	-41.3191
-16	-134.985	-16	-68.8799	-16	-40.2977
-16	-134.985	-16	-68.8799	-16	-40.2977
-18	-107.87	-18	-55.0129	-18	-35.5986
-20	-20.3021	-20	-23.9765	-20	-27.7922

Table B.3: Lateral Wall Movements of Case 3 from Three-dimensional Analysis

Case 3A		**Case 3B**		**Case 3C**	
Y	**Ux**	**Y**	**Ux**	**Y**	**Ux**
[m]	**[mm]**	**[m]**	**[mm]**	**[m]**	**[mm]**
0	-23.8156	0	-23.9199	0	-30.5904
-1	-34.3051	-1	-28.8296	-1	-32.4185
-2	-33.5098	-2	-31.8312	-2	-34.0955
-2	-33.5098	-2	-31.8312	-2	-34.0955
-2.25	-34.7303	-2.25	-32.6997	-2.25	-34.5354
-2.5	-37.4716	-2.5	-33.872	-2.5	-35.0008
-2.5	-37.4716	-2.5	-33.872	-2.5	-35.0008
-2.75	-38.5542	-2.75	-34.8412	-2.75	-35.4357
-3	-41.3601	-3	-36.0691	-3	-35.8948
-3	-41.3601	-3	-36.0691	-3	-35.8948
-4	-54.9527	-4	-41.4176	-4	-37.7544
-5	-53.8168	-5	-44.5514	-5	-39.3489
-5	-53.8168	-5	-44.5514	-5	-39.3489
-5.25	-55.9002	-5.25	-45.7639	-5.25	-39.792
-5.5	-60.1661	-5.5	-47.3832	-5.5	-40.2682
-5.5	-60.1661	-5.5	-47.3832	-5.5	-40.2682
-5.75	-61.8989	-5.75	-48.5674	-5.75	-40.6816
-6	-65.7276	-6	-50.1304	-6	-41.1306
-6	-65.7276	-6	-50.1304	-6	-41.1306

-7	-84.2182	-7	-57.12	-7	-42.9303
-8	-84.2323	-8	-60.8041	-8	-44.251
-8	-84.2323	-8	-60.8041	-8	-44.251
-8.25	-86.7798	-8.25	-62.1454	-8.25	-44.6152
-8.5	-91.8627	-8.5	-63.9539	-8.5	-45.0166
-8.5	-91.8627	-8.5	-63.9539	-8.5	-45.0166
-8.75	-94.239	-8.75	-65.1886	-8.75	-45.3296
-9	-98.6413	-9	-66.8113	-9	-45.6818
-9	-98.6413	-9	-66.8113	-9	-45.6818
-10	-118.317	-10	-73.6539	-10	-47.0262
-11	-119.02	-11	-75.8317	-11	-47.6083
-11	-119.02	-11	-75.8317	-11	-47.6083
-11.25	-122.171	-11.25	-76.6072	-11.25	-47.7571
-11.5	-127.766	-11.5	-77.8107	-11.5	-47.9439
-11.5	-127.766	-11.5	-77.8107	-11.5	-47.9439
-11.75	-130.156	-11.75	-78.3025	-11.75	-48.0172
-12	-134.074	-12	-79.1426	-12	-48.131
-12	-134.074	-12	-79.1426	-12	-48.131
-13	-150.809	-13	-82.3603	-13	-48.4698
-14	-148.086	-14	-79.4619	-14	-47.7801
-14	-148.086	-14	-79.4619	-14	-47.7801
-14.25	-147.862	-14.25	-78.6606	-14.25	-47.5752
-14.5	-149.05	-14.5	-78.2141	-14.5	-47.411
-14.5	-149.05	-14.5	-78.2141	-14.5	-47.411
-14.75	-147.978	-14.75	-77.2335	-14.75	-47.162
-15	-147.283	-15	-76.24	-15	-46.9007
-15	-147.283	-15	-76.24	-15	-46.9007
-15.5	-144.048	-15.5	-73.7434	-15.5	-46.2797
-16	-136.992	-16	-70.4409	-16	-45.5315
-16	-136.992	-16	-70.4409	-16	-45.5315
-17	-116.427	-17	-62.16	-17	-43.7387

-18	-91.7433	-18	-52.1624	-18	-41.5404
-18	-91.7433	-18	-52.1624	-18	-41.5404
-19	-65.6073	-19	-41.5343	-19	-39.1593
-20	-22.7515	-20	-28.2732	-20	-36.4864

Appendix C: Bending Moments of the Primary Wall

C.1 Plane Strain Analysis

Table C.1: Bending Moments of Primary Wall from Plane Strain Analysis

Case A		Case B		Case C	
Y	**M11**	**Y**	**M11**	**Y**	**M11**
[m]	**[kNm/m]**	**[m]**	**[kNm/m]**	**[m]**	**[kNm/m]**
0	-13.6928	0	-15.5909	0	-8.46903
0	-14.5707	0	-15.7999	0	-8.45533
-1	17.69292	-1	16.21021	-1	5.326189
-1	16.81505	-1	16.00113	-1	5.339887
-2	70.55124	-2	81.04421	-2	36.45279
-2	48.20079	-2	47.80219	-2	19.1351
-2	49.07866	-2	48.01127	-2	19.12141
-2	72.29599	-2	81.24487	-2	35.70691
-2.5	47.67137	-2.5	70.66982	-2.5	-85.8058
-2.5	45.92662	-2.5	70.46916	-2.5	-85.0599
-3	-9.45626	-3	16.5942	-3	-241.38
-3	23.04675	-3	60.09477	-3	-207.318
-3	21.30199	-3	59.89411	-3	-242.588
-3	-7.906	-3	16.59553	-3	-206.573
-4	40.05821	-4	79.7419	-4	-416.933
-4	41.60846	-4	79.74322	-4	-418.141
-5	89.57267	-5	142.8896	-5	-593.694
-5	122.2719	-5	192.4343	-5	-544.72
-5	91.12293	-5	142.8909	-5	-541.699
-5	125.1367	-5	193.235	-5	-592.486
-5.5	71.96468	-5.5	96.28881	-5.5	-743.105

-5.5	74.8295	-5.5	97.08949	-5.5	-740.084
-6	21.65749	-6	0.143287	-6	-1001.63
-6	-11.1522	-6	-56.4549	-6	-1006.71
-6	24.52231	-6	0.943965	-6	-941.49
-6	-12.9467	-6	-55.5248	-6	-938.469
-7	26.63317	-7	-124.361	-7	-1272.4
-7	24.83865	-7	-123.431	-7	-1277.47
-8	105.7115	-8	-123.351	-8	-1543.16
-8	62.62403	-8	-191.337	-8	-1471.2
-8	101.9455	-8	-125.847	-8	-1548.24
-8	64.41854	-8	-192.267	-8	-1463.52
-8.5	42.39225	-8.5	-278.075	-8.5	-1676.61
-8.5	46.15826	-8.5	-275.579	-8.5	-1684.29
-9	-13.395	-9	-427.807	-9	-1889.69
-9	-50.9158	-9	-498.461	-9	-1982.55
-9	-17.161	-9	-430.302	-9	-1897.37
-9	-49.6012	-9	-499.325	-9	-1991.29
-10	-26.1717	-10	-660.465	-10	-2228
-10	-27.4863	-10	-659.601	-10	-2236.74
-11	38.26546	-11	-742.103	-11	-2473.45
-11	-4.05682	-11	-820.741	-11	-2373.1
-11	-2.74227	-11	-821.605	-11	-2364.61
-11	34.74569	-11	-746.171	-11	-2482.19
-11.5	-59.2208	-11.5	-883.253	-11.5	-2511.42
-11.5	-62.7406	-11.5	-887.322	-11.5	-2502.93
-12	-156.707	-12	-1024.4	-12	-2641.24
-12	-186.577	-12	-1105.42	-12	-2649.74
-12	-188.323	-12	-1105.94	-12	-2761.3
-12	-160.227	-12	-1028.47	-12	-2766.58
-13	-268.934	-13	-1231.69	-13	-2803.32
-13	-267.188	-13	-1231.17	-13	-2808.61

-14	-349.545	-14	-1357.44	-14	-2845.35
-14	-319.509	-14	-1289.37	-14	-2746.94
-14	-347.799	-14	-1356.92	-14	-2850.64
-14	-321.538	-14	-1293.39	-14	-2745.14
-14.5	-366.124	-14.5	-1305.4	-14.5	-2675.37
-14.5	-364.095	-14.5	-1301.38	-14.5	-2673.56
-15	-410.71	-15	-1317.41	-15	-2619.06
-15	-417.669	-15	-1328.01	-15	-2601.99
-15	-416.661	-15	-1335.2	-15	-2603.79
-15	-408.68	-15	-1313.39	-15	-2625.52
-15.5	-420.1	-15.5	-1275.59	-15.5	-2457.16
-15.5	-419.091	-15.5	-1282.78	-15.5	-2463.62
-16	-422.53	-16	-1223.16	-16	-2301.71
-16	-421.521	-16	-1230.36	-16	-2326.16
-16	-421.214	-16	-1244.73	-16	-2295.25
-16	-424.827	-16	-1242.11	-16	-2329.95
-17	-364.299	-17	-1013.89	-17	-1823.6
-17	-360.687	-17	-1016.51	-17	-1819.81
-18	-315.732	-18	-788.755	-18	-1287.82
-18	-303.772	-18	-785.675	-18	-1313.46
-18	-313.902	-18	-790.011	-18	-1317.25
-18	-300.16	-18	-788.295	-18	-1298.85
-19	-169.474	-19	-408.875	-19	-657.967
-19	-167.644	-19	-410.132	-19	-646.94
-20	-21.3867	-20	-30.2529	-20	-17.0833
-20	-23.2167	-20	-28.9961	-20	-6.05683

C. 2 Three-dimensional Analysis

Table C.2: Bending Moments of Primary Wall of Case 1 from Three-dimensional Analysis

Case 1A	**Case 1B**	**Case 1C**

Y [m]	M_11 [kNm/m]	Y [m]	M_11 [kN/m]	Y [m]	M_11 [kN/m]
0	-14.7114	0	2.7365	0	-31.4980
-1	16.3075	-1	-31.6684	-1	30.0677
-2	126.9888	-2	13.4114	-2	198.2256
-2	47.3265	-2	-66.0733	-2	91.6333
-2.25	81.0941	-2.25	21.5908	-2.25	135.9360
-2.5	35.1994	-2.5	31.2231	-2.5	73.6464
-2.5	34.7843	-2.5	29.7701	-2.5	70.5467
-2.75	29.0151	-2.75	64.9939	-2.75	42.8050
-3	-17.1368	-3	98.7647	-3	-83.4561
-3	23.2459	-3	19.6153	-3	15.0633
-4	48.2464	-4	315.8936	-4	76.7848
-5	209.0200	-5	763.7120	-5	402.9150
-5	113.6295	-5	612.1719	-5	237.0257
-5.25	125.1697	-5.25	589.1693	-5.25	233.2495
-5.5	40.9694	-5.5	414.6266	-5.5	56.4482
-5.5	41.3194	-5.5	411.7390	-5.5	63.5840
-5.75	24.4651	-5.75	342.2204	-5.75	-48.1252
-6	7.9607	-6	171.3996	-6	-152.6986
-6	-39.3412	-6	272.7019	-6	-294.7999
-7	13.5852	-7	189.4235	-7	-274.9639
-8	66.5116	-8	207.4474	-8	-255.1280
-8	173.2891	-8	383.6757	-8	-46.6407
-8.25	86.9689	-8.25	185.7693	-8.25	-262.6711
-8.5	-0.9033	-8.5	-13.8504	-8.5	-485.3223
-8.5	0.6487	-8.5	-12.1372	-8.5	-478.7014
-8.75	-14.8630	-8.75	-99.4136	-8.75	-624.7290
-9	-28.8227	-9	-291.7706	-9	-764.1356
-9	-81.3189	-9	-184.9769	-9	-920.9970
-10	-6.0763	-10	-338.9536	-10	-989.2546

-11	191.2185	-11	-386.1366	-11	-832.5774
-11	69.1663	-11	-211.3071	-11	-1057.5123
-11.25	70.8132	-11.25	-397.1614	-11.25	-1035.2350
-11.5	-49.5920	-11.5	-583.0157	-11.5	-1237.8926
-11.5	-52.1171	-11.5	-583.9292	-11.5	-1243.0805
-11.75	-91.1949	-11.75	-678.1057	-11.75	-1376.9974
-12	-130.2726	-12	-772.2823	-12	-1510.9142
-12	-168.7210	-12	-864.0926	-12	-1643.3401
-13	-225.2419	-13	-992.8909	-13	-1767.1600
-14	-201.2728	-14	-978.8070	-14	-1701.2541
-14	-281.7628	-14	-1121.6891	-14	-1890.9799
-14.25	-251.0131	-14.25	-1034.3808	-14.25	-1750.9970
-14.5	-300.7534	-14.5	-1102.6373	-14.5	-1800.7400
-14.5	-306.3188	-14.5	-1089.9545	-14.5	-1816.7964
-14.75	-322.7066	-14.75	-1118.4809	-14.75	-1826.2801
-15	-339.0943	-15	-1148.0842	-15	-1835.7638
-15	-347.7292	-15	-1134.3245	-15	-1848.8798
-15.5	-346.0999	-15.5	-1115.0942	-15.5	-1774.7964
-16	-343.4019	-16	-1090.9382	-16	-1711.3699
-16	-344.4706	-16	-1082.1042	-16	-1700.7129
-17	-292.2230	-17	-878.0332	-17	-1337.5694
-18	-258.6457	-18	-665.1282	-18	-954.0039
-18	-241.0442	-18	-663.1903	-18	-963.7689
-19	-141.3603	-19	-340.9618	-19	-481.4579
-20	-24.0748	-20	-18.7334	-20	-8.9119

Table C.3: Bending Moments of Primary Wall of Case 2 from Three-dimensional Analysis

Case 2A		**Case 2B**		**Case 2C**	
Y	**M_11**	**Y**	**M_11**	**Y**	**M_11**
[m]	**[kNm/m]**	**[m]**	**[kN/m]**	**[m]**	**[kN/m]**

0	-16.3093	0	-15.5067	0	-9.1552
-1	12.9373	-1	7.2525	-1	-0.5886
-2	78.9144	-2	30.0117	-2	50.2816
-2	42.1838	-2	87.7328	-2	7.9781
-2.25	64.0293	-2.25	93.0753	-2.25	17.4171
-2.5	49.7311	-2.5	98.4177	-2.5	-15.4475
-2.5	49.1442	-2.5	97.2828	-2.5	-13.7601
-2.75	43.0418	-2.75	107.7336	-2.75	-42.1964
-3	36.3525	-3	118.1843	-3	-70.6327
-3	-4.7240	-3	64.0278	-3	-117.3426
-4	45.8792	-4	176.9515	-4	-170.5078
-5	146.3090	-5	365.1537	-5	-223.6730
-5	96.4823	-5	289.8753	-5	-156.4826
-5.25	113.4785	-5.25	315.2029	-5.25	-251.8149
-5.5	80.8283	-5.5	269.0864	-5.5	-345.1180
-5.5	80.6479	-5.5	265.2522	-5.5	-347.1473
-5.75	61.6236	-5.75	227.9073	-5.75	-432.6442
-6	42.4190	-6	186.7283	-6	-520.1703
-6	-7.8991	-6	110.7427	-6	-592.9579
-7	22.5270	-7	59.9454	-7	-829.2120
-8	112.4735	-8	104.3729	-8	-967.5776
-8	52.9531	-8	9.1482	-8	-1065.4661
-8.25	77.8890	-8.25	17.5938	-8.25	-1096.0554
-8.5	43.3045	-8.5	-65.2190	-8.5	-1219.9596
-8.5	41.1136	-8.5	-69.1854	-8.5	-1224.5333
-8.75	22.0760	-8.75	-141.1866	-8.75	-1337.1781
-9	3.0385	-9	-309.5405	-9	-1557.8552
-9	-47.0459	-9	-217.1543	-9	-1454.3966
-10	-13.1929	-10	-473.6620	-10	-1860.9908
-11	79.2955	-11	-534.1449	-11	-2164.1265
-11	20.6601	-11	-637.7835	-11	-2037.2924

-11.25	21.4217	-11.25	-625.5217	-11.25	-2138.8161
-11.5	-36.4521	-11.5	-712.6478	-11.5	-2240.3397
-11.5	-40.6998	-11.5	-716.8984	-11.5	-2233.5278
-11.75	-84.8576	-11.75	-792.8134	-11.75	-2320.6294
-12	-129.0154	-12	-981.7506	-12	-2407.7309
-12	-168.1082	-12	-872.9789	-12	-2555.0646
-13	-256.7217	-13	-1141.3752	-13	-2684.6386
-14	-300.5539	-14	-1300.9999	-14	-2814.2127
-14	-345.3352	-14	-1197.1617	-14	-2678.1884
-14.25	-331.6094	-14.25	-1219.4395	-14.25	-2671.4659
-14.5	-362.6649	-14.5	-1241.7172	-14.5	-2701.1873
-14.5	-368.8428	-14.5	-1264.9410	-14.5	-2664.7434
-14.75	-387.9690	-14.75	-1270.5201	-14.75	-2671.8095
-15	-395.8256	-15	-1276.0993	-15	-2642.4316
-15	-407.0952	-15	-1234.5077	-15	-2572.3658
-15.5	-394.8442	-15.5	-1190.4408	-15.5	-2443.7241
-16	-393.8628	-16	-1340.2058	-16	-2315.0824
-16	-482.5237	-16	-1146.3739	-16	-2646.7725
-18	-277.1344	-18	-746.6196	-18	-1455.7487
-20	-71.7451	-20	-153.0333	-20	-264.7249

Table C.4: Bending Moments of Primary Wall of Case 3 from Three-dimensional Analysis

Case 3A		**Case 3B**		**Case 3C**	
Y	**M_11**	**Y**	**M_11**	**Y**	**M_11**
[m]	**[kNm/m]**	**[m]**	**[kN/m]**	**[m]**	**[kN/m]**
0	-9.0027	0	-12.6110	0	-7.4894
-1	18.6430	-1	11.1386	-1	4.8383
-2	46.2887	-2	34.8882	-2	17.1659
-2	63.3831	-2	77.6340	-2	54.3047
-2.25	47.0723	-2.25	80.5440	-2.25	29.1503

-2.5	32.0194	-2.5	84.9217	-2.5	7.9525
-2.5	30.7616	-2.5	83.4540	-2.5	3.9958
-2.75	26.2988	-2.75	93.8361	-2.75	-12.4713
-3	20.5782	-3	102.7505	-3	-32.8952
-3	-0.4233	-3	61.9304	-3	-74.3192
-4	49.0227	-4	168.4715	-4	-94.6920
-5	122.8967	-5	332.6164	-5	-58.0173
-5	98.4686	-5	275.0126	-5	-115.0647
-5.25	88.7850	-5.25	281.9075	-5.25	-141.3075
-5.5	55.3231	-5.5	235.1253	-5.5	-216.4430
-5.5	54.6734	-5.5	231.1986	-5.5	-224.5976
-5.75	38.6568	-5.75	195.2756	-5.75	-290.4391
-6	21.9905	-6	97.0007	-6	-429.4210
-6	-2.1168	-6	155.4259	-6	-364.4353
-7	31.4968	-7	49.9502	-7	-613.0876
-8	65.1104	-8	2.8997	-8	-796.7541
-8	93.7949	-8	74.7856	-8	-719.3696
-8.25	57.3549	-8.25	-10.4194	-8.25	-837.9969
-8.5	20.4919	-8.5	-95.6244	-8.5	-956.6243
-8.5	20.9150	-8.5	-92.6357	-8.5	-947.6811
-8.75	4.2396	-8.75	-164.1718	-8.75	-1,052.8853
-9	-12.0126	-9	-235.7080	-9	-1,158.0895
-9	-34.8048	-9	-302.8705	-9	-1,247.0743
-10	3.9964	-10	-453.2118	-10	-1,509.8060
-11	70.9539	-11	-525.3639	-11	-1,678.0689
-11	42.7977	-11	-603.5531	-11	-1,772.5378
-11.25	9.8320	-11.25	-616.0763	-11.25	-1,784.6159
-11.5	-52.1333	-11.5	-706.7887	-11.5	-1,891.1630
-11.5	-51.2899	-11.5	-705.2538	-11.5	-1,883.0358
-11.75	-94.9676	-11.75	-781.0249	-11.75	-1,972.0968
-12	-152.1517	-12	-928.4140	-12	-2,166.7700

-12	-137.8019	-12	-856.7960	-12	-2,061.1579
-13	-242.9107	-13	-1,079.7035	-13	-2,319.1105
-14	-333.6698	-14	-1,230.9930	-14	-2,471.4511
-14	-312.8145	-14	-1,151.2697	-14	-2,361.3007
-14.25	-345.5430	-14.25	-1,175.9934	-14.25	-2,369.7917
-14.5	-381.0142	-14.5	-1,215.5740	-14.5	-2,399.8004
-14.5	-378.2715	-14.5	-1,200.7172	-14.5	-2,378.2828
-14.75	-400.1433	-14.75	-1,222.9276	-14.75	-2,385.0661
-15	-427.3248	-15	-1,245.1314	-15	-2,391.0111
-15	-419.2723	-15	-1,230.2811	-15	-2,370.3318
-15.5	-430.0849	-15.5	-1,204.0471	-15.5	-2,286.4250
-16	-432.8450	-16	-1,162.9629	-16	-2,181.8389
-16	-433.7121	-16	-1,172.5307	-16	-2,209.7183
-17	-368.2541	-17	-955.9624	-17	-1,788.2059
-18	-325.7034	-18	-751.0698	-18	-1,383.8829
-18	-302.7960	-18	-739.3941	-18	-1,366.6935
-19	-179.0881	-19	-393.4783	-19	-724.2404
-20	-32.4728	-20	-35.8867	-20	-64.5979

C.3 Maximum Wall Bending Moments

Table C.5: Maximum Bending Moments of Primary Wall

Analysis	**Case**	**Maximum Wall Bending Moment (kNm/m)**
2D	A	-424.827
	B	-1357.44
	C	-2850.64
3D	1A	-347.73
	1B	-1148.08
	1C	-1890.98
	2A	-482.52
	2B	-1340.21

	2C	-2814.21
	3A	-433.71
	3B	-1245.13
	3C	-2471.45

Appendix D: Earth Pressure on the Primary Walls

D.1 Lateral Earth Pressure Charts

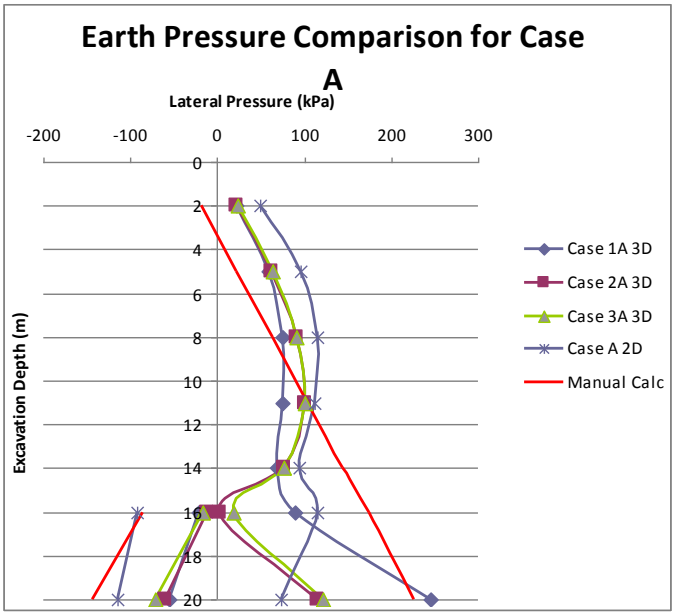

Figure D.1: Lateral Earth Pressure Diagram for Cases of Flexible Wall

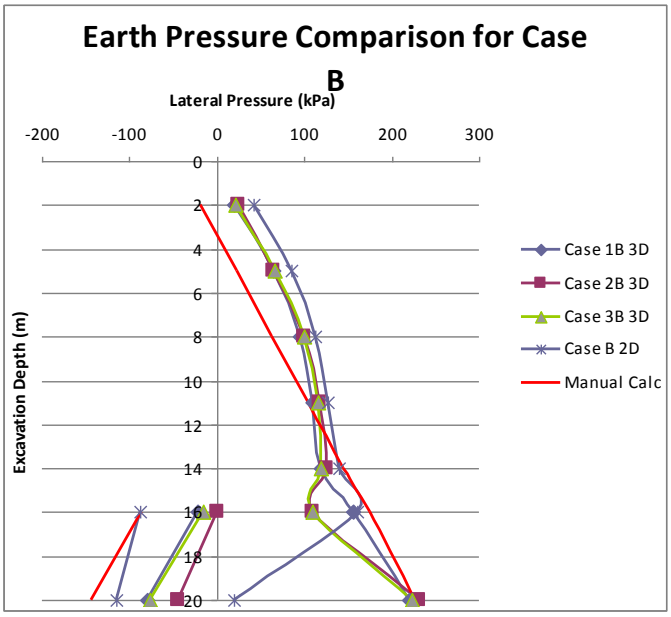

Figure D.2: Lateral Earth Pressure Diagram for Cases of Medium Flexible Wall

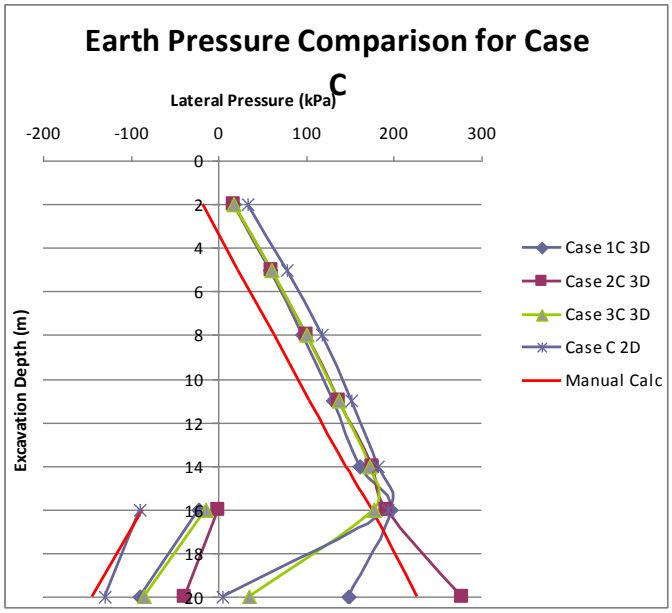

Figure D.3: Lateral Earth Pressure Diagram for Cases of Stiff Wall

D.2 Tables of Lateral Earth Pressure

The tables of lateral earth pressure for plane strain and three-dimensional analysis are presented on the next pages.

Table D.1: Lateral Earth Pressure from Plane Strain Analysis

Case A			**Case B**			**Case C**			**Lateral Pressure from Manual Calculations**
Active Pressure			**Active Pressure**			**Active Pressure**			
Stress Points No	**Y**	**s' xx**	**Stress Points No**	**Y**	**s' xx**	**Stress Points No**	**Y**	**s' xx**	
	[m]	**[kN/m^2]**		**[m]**	**[kN/m^2]**		**[m]**	**[kN/m^2]**	**[kN/m^2]**
1311	-2.014	49.577	1311	-2.014	41.288	963	-2.203	33.269	-12.607
1287	-5.063	95.568	951	-5.175	85.619	1287	-5.063	78.152	28.857
1275	-8.014	114.437	1275	-8.014	112.043	1275	-8.014	117.284	68.994
927	-11.124	112.647	1227	-10.964	127.101	1227	-10.964	152.069	111.291
915	-14.057	94.165	915	-14.057	139.898	915	-14.057	181.605	151.176
902	-15.967	115.512	902	-15.967	160.043	902	-15.967	193.251	177.148
974	-19.874	73.993	974	-19.874	18.868	974	-19.874	4.277	230.284
Passive Pressure			**Passive Pressure**			**Passive Pressure**			**Lateral Pressure from Manual Calculations**
Stress Points No	**Y**	**s' xx**	**Stress Points No**	**Y**	**s' xx**	**Stress Points No**	**Y**	**s' xx**	
	[m]	**[kN/m^2]**		**[m]**	**[kN/m^2]**		**[m]**	**[kN/m^2]**	**[kN/m^2]**
2439	-16.126	-92.557	2439	-16.126	-87.538	2439	-16.126	-90.221	-80.722
2426	-19.874	-115.509	2426	-19.874	-114.424	2426	-19.874	-130.121	-149.678

Table D.2: Lateral Earth Pressure from Case 1 of Three-dimensional Analysis

Case 1A			**Case 1B**			**Case 1C**			**Lateral Pressure from Manual Calculations**
Active Pressure			**Active Pressure**			**Active Pressure**			
Stress Points No	**Y**	**σ_3'**	**Stress Points No**	**Y**	**σ_3'**	**Stress Points No**	**Y**	**σ_3'**	
	[m]	**[kN/m^2]**		**[m]**	**[kN/m^2]**		**[m]**	**[kN/m^2]**	**[kN/m^2]**
73	-1.577	21.10108	85	-1.577	18.994	73	-1.577	17.567	-18.548
8317	-4.577	58.20608	8401	-4.577	63.628	8317	-4.577	58.365	22.252
16561	-7.577	74.56654	16717	-7.577	94.558	16561	-7.577	95.618	63.052
24805	-10.577	74.41656	25033	-10.577	109.276	24805	-10.577	129.954	103.852
33049	-13.577	68.20125	33349	-13.577	119.196	33049	-13.577	160.540	144.652
41293	-15.789	89.97269	41665	-15.789	156.453	41293	-15.789	195.936	174.726
46789	-19.577	245.7857	47209	-19.577	219.098	46789	-19.577	147.737	226.252
Passive Pressure			**Passive Pressure**			**Passive Pressure**			**Lateral Pressure from Manual Calculations**
Stress Points No	**Y**	**σ_3'**	**Stress Points No**	**Y**	**σ_3'**	**Stress Points No**	**Y**	**σ_3'**	
	[m]	**[kN/m^2]**		**[m]**	**[kN/m^2]**		**[m]**	**[kN/m^2]**	**[kN/m^2]**
46696	-16.423	-21.703	47104	-16.423	-21.753	46696	-16.423	-22.801	-86.177
49441	-19.577	-55.571	49873	-19.577	-79.707	49441	-19.577	-90.014	-144.223

Table D.3: Lateral Earth Pressure from Case 2 of Three-dimensional Analysis

Case 2A			**Case 2B**			**Case 2C**			**Lateral Pressure from Manual Calculations**
Active Pressure			**Active Pressure**			**Active Pressure**			
Stress Points No	**Y**	**σ_3'**	**Stress Points No**	**Y**	**σ_3'**	**Stress Points No**	**Y**	**σ_3'**	
	[m]	**[kN/m^2]**		**[m]**	**[kN/m^2]**		**[m]**	**[kN/m^2]**	**[kN/m^2]**
39	-1.577	21.710	147	-1.577	24.469	39	-1.577	17.355	-18.548
5619	-4.577	62.580	5619	-4.577	64.399	5619	-4.577	59.664	22.252
11199	-7.577	91.709	11199	-7.577	100.102	11199	-7.577	99.864	63.052
16779	-10.577	100.588	16779	-10.577	117.918	16779	-10.577	137.580	103.852
22359	-13.577	77.037	22359	-13.577	124.761	22359	-13.577	175.014	144.652
27939	-15.789	2.296	27939	-15.789	108.816	27939	-15.789	192.110	174.726
29799	-19.155	115.663	29799	-19.155	230.801	29799	-19.155	277.923	220.504
Passive Pressure			**Passive Pressure**			**Passive Pressure**			**Lateral Pressure from Manual Calculations**
Stress Points No	**Y**	**σ_3'**	**Stress Points No**	**Y**	**σ_3'**	**Stress Points No**	**Y**	**σ_3'**	
	[m]	**[kN/m^2]**		**[m]**	**[kN/m^2]**		**[m]**	**[kN/m^2]**	**[kN/m^2]**
31620	-16.845	-12.366	31620	-16.845	0.000	31620	-16.845	0.000	-93.954
31615	-19.155	-59.973	31615	-19.155	-43.914	31615	-19.155	-39.288	-136.446

Table D.4: Lateral Earth Pressure from Case 3 of Three-dimensional Analysis

Case 3A			**Case 3B**			**Case 3C**			**Lateral Pressure from Manual Calculations**
Active Pressure			**Active Pressure**			**Active Pressure**			
Stress Points No	**Y**	**σ_3'**	**Stress Points No**	**Y**	**σ_3'**	**Stress Points No**	**Y**	**σ_3'**	
	[m]	**[kN/m^2]**		**[m]**	**[kN/m^2]**		**[m]**	**[kN/m^2]**	**[kN/m^2]**
27	-1.577	22.906	27	-1.577	21.002	27	-1.577	16.996	-18.548
5499	-4.577	63.927	5499	-4.577	66.239	5499	-4.577	59.958	22.252
10971	-7.577	91.166	10971	-7.577	100.409	10971	-7.577	100.127	63.052
16443	-10.577	100.484	16443	-10.577	116.238	16443	-10.577	137.428	103.852
21915	-13.577	76.977	21915	-13.577	118.843	21915	-13.577	171.594	144.652
27387	-15.789	18.077	27387	-15.789	110.040	27387	-15.789	177.132	174.726
31035	-19.577	121.638	31035	-19.577	223.686	31035	-19.577	35.023	226.252
Passive Pressure			**Passive Pressure**			**Passive Pressure**			**Lateral Pressure from Manual Calculations**
Stress Points No	**Y**	**σ_3'**	**Stress Points No**	**Y**	**σ_3'**	**Stress Points No**	**Y**	**σ_3'**	
	[m]	**[kN/m^2]**		**[m]**	**[kN/m^2]**		**[m]**	**[kN/m^2]**	**[kN/m^2]**
31006	-16.423	-16.429	31006	-16.423	-16.200	31006	-16.423	-15.088	-86.177
32827	-19.577	-71.034	32827	-19.577	-77.179	32827	-19.577	-84.575	-144.223

Appendix E: Strut Loads

E.1 Calculation of Pressures on Struts based on Peck's APD

In soft clay, $c_u = 20 + 1.2z$. Therefore, the average c_u for the depth 0 m to 16 m is:

$$c_{u,avg} = \frac{(20 + 1.2 * 0) + (20 + 1.2 * 16)}{2} = 29.6kPa$$

With $\gamma = 16kN/m^3$, the stability number:

$$\frac{\gamma H}{c} = \frac{16 * 16}{29.6} = 8.648 > 4$$

Since the stability number is larger than 4, use the apparent pressure diagram for soft/medium clay below.

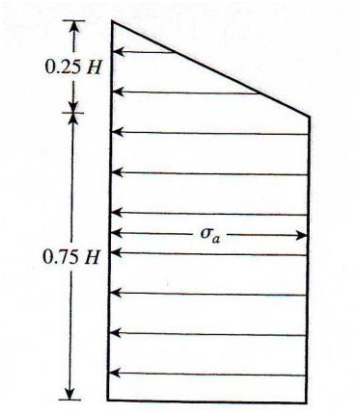

Figure E.1: Apparent Pressure Diagram for Soft or Medium Clay

$$\sigma_a = \gamma H\left[1 - \frac{4c}{\gamma H}\right] = 16 * 16 * \left[1 - \frac{4 * 29.6}{16 * 16}\right] = 137.6kPa$$

E.2 Calculating Strut Forces to Equivalent Horizontal Pressures

The maximum pressure on each strut is calculated by dividing the maximum strut forces to area extending horizontally at half the distance to the next vertical row of struts on each side, and vertically half the distance to the horizontal sets of struts immediately above and below.

Below are examples of calculation of strut forces to pressures from the plane strain analysis result.

1. Level 2 m strut, F = 856.807 kN (in compression)

$$\text{Pressure} = \frac{F}{A} = \frac{856.807kN}{(3.5m)*(5m)} = 48.96kPa$$

2. Level 5 m strut, F = 1671.254 kN (in compression)

$$\text{Pressure} = \frac{F}{A} = \frac{1671.254kN}{(3m)*(5m)} = 111.417kPa$$

3. Level 8 m strut, F = 1961.161 kN (in compression)

$$\text{Pressure} = \frac{F}{A} = \frac{1961.161kN}{(3m)*(5m)} = 130.744kPa$$

4. Level 11 m strut, F = 2367.621 kN (in compression)

$$\text{Pressure} = \frac{F}{A} = \frac{2367.621kN}{(3m)*(5m)} = 157.841kPa$$

5. Level 14 m, F = 769.171 kN (in compression)

$$\text{Pressure} = \frac{F}{A} = \frac{769.171kN}{(2.5m)*(5m)} = 61.534kPa$$

Pressures for other cases are calculated using the similar manner.

E.3 Tables of Strut Forces and Pressures Compared to Peck's APD

Tables of maximum strut forces and maximum pressures from plane strain and three-dimensional analyses are presented on the next pages.

Table E.1: Strut Forces and Pressures from Plane Strain Analysis

Case A			Case B			Case C		
Level	**Force***	**Pressure**	**Level**	**Force***	**Pressure**	**Level**	**Force***	**Pressure**
(m)	**(kN)**	**(kPa)**	**(m)**	**(kN)**	**(kPa)**	**(m)**	**(kN)**	**(kPa)**
0	0	0	0	0	0	0	0	0
-2	856.807	48.960	-2	1019.660	58.266	-2	1456.738	83.242
-5	1671.254	111.417	-5	2186.233	145.749	-5	2066.968	137.798
-8	1961.161	130.744	-8	2126.891	141.793	-8	2449.855	163.324
-11	2367.621	157.841	-11	2162.849	144.190	-11	2730.632	182.042
-14	769.171	61.534	-14	850.380	68.030	-14	874.203	69.936
-16	0	0	-16	0	0	-16	0	0

* in compression

Table E.2: Strut Forces and Pressures of Case 1 from Three-dimensional Analysis

Case 1A			Case 1B			Case 1C		
Level	**Force***	**Pressure**	**Level**	**Force***	**Pressure**	**Level**	**Force***	**Pressure**
(m)	**(kN)**	**(kPa)**	**(m)**	**(kN)**	**(kPa)**	**(m)**	**(kN)**	**(kPa)**
0	0	0	0	0	0	0	0	0
-2	754.240	43.099	-2	638.980	36.513	-2	1414.172	80.810
-5	1370.120	91.341	-5	2286.478	152.432	-5	1850.082	123.339
-8	1457.460	97.164	-8	2061.700	137.447	-8	2051.635	136.776
-11	1724.660	114.977	-11	1772.019	118.135	-11	1849.928	123.329
-14	595.573	47.646	-14	564.948	45.196	-14	653.489	52.279
-16	0	0	-16	0	0	-16	0	0

* in compression

Table E.3: Strut Forces and Pressures of Case 2 from Three-dimensional Analysis

Case 2A			Case 2B			Case 2C		
Level	**Force***	**Pressure**	**Level**	**Force***	**Pressure**	**Level**	**Force***	**Pressure**
(m)	**(kN)**	**(kPa)**	**(m)**	**(kN)**	**(kPa)**	**(m)**	**(kN)**	**(kPa)**

0	0	0	0	0	0	0	0	0
-2	813.760	46.501	-2	1019.420	58.253	-2	1466.550	83.803
-5	1539.460	102.631	-5	2187.566	145.838	-5	2074.262	138.284
-8	1655.000	110.333	-8	2169.518	144.635	-8	2065.467	137.698
-11	1955.520	130.368	-11	1787.180	119.145	-11	1446.243	96.416
-14	632.148	50.572	-14	493.947	39.516	-14	387.602	31.008
-16	0	0	-16	0	0	-16	0	0

* in compression

Table E.4: Strut Forces and Pressures of Case 3 from Three-dimensional Analysis

Case 3A			**Case 3B**			**Case 3C**		
Level (m)	**Force* (kN)**	**Pressure (kPa)**	**Level (m)**	**Force* (kN)**	**Pressure (kPa)**	**Level (m)**	**Force* (kN)**	**Pressure (kPa)**
0	0	0	0	0	0	0	0	0
-2	832.380	47.565	-2	1034.280	59.102	-2	1482.820	84.733
-5	1531.320	102.088	-5	2167.690	144.513	-5	2017.368	134.491
-8	1677.980	111.865	-8	2142.252	142.817	-8	2103.628	140.242
-11	2035.700	135.713	-11	1786.858	119.124	-11	1720.571	114.705
-14	624.890	49.991	-14	535.052	42.804	-14	532.907	42.633
-16	0	0	-16	0	0	-16	0	0

* in compression

Appendix F: Lateral Movements of the Secondary Wall

Table F.1: Lateral Wall Movements of Case 1

Case 1A		**Case 1B**		**Case 1C**	
Y	**Uz**	**Y**	**Uz**	**Y**	**Uz**
[m]	**[mm]**	**[m]**	**[mm]**	**[m]**	**[mm]**
0	21.22852	0	15.45052	0	12.13836
-1	24.18972	-1	18.26856	-1	13.85731
-2	24.49527	-2	20.8626	-2	15.56619
-2	24.49527	-2	20.8626	-2	15.56619
-2.25	24.8718	-2.25	21.55732	-2.25	15.99528
-2.5	24.98604	-2.5	22.14693	-2.5	16.41363
-2.5	24.98604	-2.5	22.14693	-2.5	16.41363
-2.75	25.34645	-2.75	22.75065	-2.75	16.84537
-3	27.11146	-3	23.55667	-3	17.29557
-3	27.11146	-3	23.55667	-3	17.29557
-4	34.43006	-4	26.68059	-4	19.06771
-5	36.66931	-5	29.43854	-5	20.80004
-5	36.66931	-5	29.43854	-5	20.80004
-5.25	37.3999	-5.25	30.15463	-5.25	21.2306
-5.5	38.29002	-5.5	30.86267	-5.5	21.65737
-5.5	38.29002	-5.5	30.86267	-5.5	21.65737
-5.75	39.63069	-5.75	31.80721	-5.75	22.12214
-6	42.58559	-6	33.00414	-6	22.60918
-6	42.58559	-6	33.00414	-6	22.60918
-7	54.79876	-7	37.76168	-7	24.49991
-8	59.34471	-8	41.77069	-8	26.26328
-8	59.34471	-8	41.77069	-8	26.26328
-8.25	60.59546	-8.25	42.75364	-8.25	26.6886

-8.5	62.14737	-8.5	43.74041	-8.5	27.10895
-8.5	62.14737	-8.5	43.74041	-8.5	27.10895
-8.75	64.02394	-8.75	44.94053	-8.75	27.56225
-9	67.52233	-9	46.38378	-9	28.03458
-9	67.52233	-9	46.38378	-9	28.03458
-10	81.25299	-10	51.73425	-10	29.79651
-11	86.11093	-11	55.35924	-11	31.26953
-11	86.11093	-11	55.35924	-11	31.26953
-11.25	87.22405	-11.25	56.12154	-11.25	31.60289
-11.5	88.59754	-11.5	56.85561	-11.5	31.92609
-11.5	88.59754	-11.5	56.85561	-11.5	31.92609
-11.75	90.58658	-11.75	57.68385	-11.75	32.26462
-12	94.05623	-12	58.69706	-12	32.6168
-12	94.05623	-12	58.69706	-12	32.6168
-13	106.2615	-13	61.73315	-13	33.82215
-14	107.9433	-14	61.7955	-14	34.56602
-14	107.9433	-14	61.7955	-14	34.56602
-14.25	107.7915	-14.25	61.55543	-14.25	34.70467
-14.5	107.7448	-14.5	61.25565	-14.5	34.82971
-14.5	107.7448	-14.5	61.25565	-14.5	34.82971
-14.75	107.3096	-14.75	60.82377	-14.75	34.9375
-15	107.0985	-15	60.37001	-15	35.03668
-15	107.0985	-15	60.37001	-15	35.03668
-15.5	105.0773	-15.5	58.93911	-15.5	35.15243
-16	100.6198	-16	56.9109	-16	35.17923
-16	100.6198	-16	56.9109	-16	35.17923
-17	86.66939	-17	51.37138	-17	35.00575
-18	68.77187	-18	44.18733	-18	34.55633
-18	68.77187	-18	44.18733	-18	34.55633
-19	47.20698	-19	35.94522	-19	33.93936
-20	18.31265	-20	26.60334	-20	33.21571

Table F.2: Lateral Wall Movements of Case 2

Case 2A		**Case 2B**		**Case 2C**	
Y	**Uz**	**Y**	**Uz**	**Y**	**Uz**
[m]	**[mm]**	**[m]**	**[mm]**	**[m]**	**[mm]**
0	26.38443	0	16.52789	0	14.11192
-1	30.87086	-1	20.24572	-1	16.15024
-2	31.20581	-2	23.4997	-2	18.15907
-2	31.20581	-2	23.4997	-2	18.15907
-2.25	31.59786	-2.25	24.42066	-2.25	18.64484
-2.5	30.95214	-2.5	25.01969	-2.5	19.09186
-2.5	30.95214	-2.5	25.01969	-2.5	19.09186
-2.75	31.65329	-2.75	25.80249	-2.75	19.60942
-3	34.51845	-3	27.00251	-3	20.17262
-3	34.51845	-3	27.00251	-3	20.17262
-4	42.68914	-4	31.15254	-4	22.29529
-5	46.3473	-5	35.01391	-5	24.35528
-5	46.3473	-5	35.01391	-5	24.35528
-5.25	47.09559	-5.25	35.8064	-5.25	24.80705
-5.5	47.09562	-5.5	36.36339	-5.5	25.22344
-5.5	47.09562	-5.5	36.36339	-5.5	25.22344
-5.75	49.11031	-5.75	37.54934	-5.75	25.73659
-6	53.57494	-6	39.20143	-6	26.29276
-6	53.57494	-6	39.20143	-6	26.29276
-7	66.86274	-7	44.77104	-7	28.31104
-8	72.99381	-8	49.59832	-8	30.10931
-8	72.99381	-8	49.59832	-8	30.10931
-8.25	74.15907	-8.25	50.52216	-8.25	30.47083
-8.5	74.66638	-8.5	51.21343	-8.5	30.79042
-8.5	74.66638	-8.5	51.21343	-8.5	30.79042
-8.75	77.26286	-8.75	52.5594	-8.75	31.19565

-9	82.35261	-9	54.35154	-9	31.6355
-9	82.35261	-9	54.35154	-9	31.6355
-10	97.07353	-10	59.90747	-10	33.06144
-11	103.2771	-11	63.68525	-11	34.04956
-11	103.2771	-11	63.68525	-11	34.04956
-11.25	104.0817	-11.25	64.24167	-11.25	34.19961
-11.5	104.1498	-11.5	64.51824	-11.5	34.2982
-11.5	104.1498	-11.5	64.51824	-11.5	34.2982
-11.75	106.6178	-11.75	65.26161	-11.75	34.4407
-12	111.3715	-12	66.38358	-12	34.60998
-12	111.3715	-12	66.38358	-12	34.60998
-13	122.4036	-13	68.52074	-13	34.84916
-14	123.3455	-14	67.5912	-14	34.47406
-14	123.3455	-14	67.5912	-14	34.47406
-14.25	122.8791	-14.25	67.05767	-14.25	34.30639
-14.5	121.3952	-14.5	66.19074	-14.5	34.08371
-14.5	121.3952	-14.5	66.19074	-14.5	34.08371
-14.75	120.0756	-14.75	65.28059	-14.75	33.84446
-15	120.1754	-15	64.63642	-15	33.62583
-15	120.1754	-15	64.63642	-15	33.62583
-15.5	116.6734	-15.5	62.38264	-15.5	33.03979
-16	113.3308	-16	60.21317	-16	32.4422
-16	113.3308	-16	60.21317	-16	32.4422
-18	86.42185	-18	46.73811	-18	29.09635
-20	18.63748	-20	21.32494	-20	23.81195

Table F.3:Lateral Wall Movements of Case 3

Case 3A		**Case 3B**		**Case 3C**	
Y	**Uz**	**Y**	**Uz**	**Y**	**Uz**
[m]	**[mm]**	**[m]**	**[mm]**	**[m]**	**[mm]**

0	30.90565	0	17.5744	0	16.78279
-1	35.1336	-1	21.60284	-1	18.88283
-2	33.25615	-2	24.87482	-2	20.92618
-2	33.25615	-2	24.87482	-2	20.92618
-2.25	33.96245	-2.25	25.97865	-2.25	21.44757
-2.5	31.95601	-2.5	26.36161	-2.5	21.87995
-2.5	31.95601	-2.5	26.36161	-2.5	21.87995
-2.75	31.57718	-2.75	27.04665	-2.75	22.39526
-3	35.09966	-3	28.55182	-3	23.0055
-3	35.09966	-3	28.55182	-3	23.0055
-4	42.84253	-4	33.01174	-4	25.19356
-5	46.71162	-5	37.22825	-5	27.32678
-5	46.71162	-5	37.22825	-5	27.32678
-5.25	48.32331	-5.25	38.31111	-5.25	27.82704
-5.5	47.38875	-5.5	38.74555	-5.5	28.24176
-5.5	47.38875	-5.5	38.74555	-5.5	28.24176
-5.75	48.47063	-5.75	39.80536	-5.75	28.74806
-6	53.6786	-6	41.72923	-6	29.34671
-6	53.6786	-6	41.72923	-6	29.34671
-7	66.75	-7	47.49418	-7	31.43343
-8	73.26426	-8	52.47942	-8	33.30671
-8	73.26426	-8	52.47942	-8	33.30671
-8.25	75.29497	-8.25	53.64088	-8.25	33.71659
-8.5	74.84066	-8.5	54.15173	-8.5	34.03457
-8.5	74.84066	-8.5	54.15173	-8.5	34.03457
-8.75	76.47296	-8.75	55.30396	-8.75	34.43393
-9	82.22309	-9	57.29357	-9	34.91758
-9	82.22309	-9	57.29357	-9	34.91758
-10	96.34834	-10	62.74833	-10	36.43317
-11	102.8035	-11	66.41571	-11	37.53351
-11	102.8035	-11	66.41571	-11	37.53351

-11.25	104.4617	-11.25	67.14875	-11.25	37.73631
-11.5	103.5456	-11.5	67.18311	-11.5	37.83903
-11.5	103.5456	-11.5	67.18311	-11.5	37.83903
-11.75	104.9655	-11.75	67.66858	-11.75	37.99313
-12	110.3024	-12	68.92946	-12	38.22513
-12	110.3024	-12	68.92946	-12	38.22513
-13	120.7779	-13	70.82127	-13	38.63186
-14	121.9002	-14	69.69425	-14	38.45635
-14	121.9002	-14	69.69425	-14	38.45635
-14.25	122.3718	-14.25	69.32074	-14.25	38.36561
-14.5	119.8972	-14.5	68.18235	-14.5	38.16941
-14.5	119.8972	-14.5	68.18235	-14.5	38.16941
-14.75	117.6375	-14.75	67.05545	-14.75	37.96873
-15	118.3051	-15	66.57008	-15	37.83611
-15	118.3051	-15	66.57008	-15	37.83611
-15.5	114.51	-15.5	64.15471	-15.5	37.35821
-16	110.0369	-16	61.48759	-16	36.8139
-16	110.0369	-16	61.48759	-16	36.8139
-17	94.90841	-17	54.44703	-17	35.42143
-18	75.41	-18	45.73092	-18	33.70348
-18	75.41	-18	45.73092	-18	33.70348
-19	52.36924	-19	35.84726	-19	31.77092
-20	20.45186	-20	24.44873	-20	29.66204

Appendix G: Lateral Movements of the Primary Wall after Lowest Strut Failure Condition

G.1 Plane Strain Analysis

Table G.1: Lateral Wall Movements after Strut Failure from Plane Strain Analysis

Case A		Case B		Case C	
Y	**Ux**	**Y**	**Ux**	**Y**	**Ux**
[m]	**[mm]**	**[m]**	**[mm]**	**[m]**	**[mm]**
0	-24.899	0	-24.476	0	-24.619
-0.5	-26.941	-0.5	-26.250	-0.5	-25.901
-1	-29.012	-1	-28.028	-1	-27.184
-1.5	-31.194	-1.5	-29.816	-1.5	-28.468
-2	-33.618	-2	-31.626	-2	-29.754
-2	-33.618	-2	-31.626	-2	-29.754
-2.25	-34.994	-2.25	-32.545	-2.25	-30.398
-2.5	-36.449	-2.5	-33.474	-2.5	-31.043
-2.75	-37.960	-2.75	-34.411	-2.75	-31.690
-3	-39.510	-3	-35.359	-3	-32.340
-3	-39.510	-3	-35.359	-3	-32.340
-3.5	-42.685	-3.5	-37.291	-3.5	-33.650
-4	-45.948	-4	-39.283	-4	-34.980
-4.5	-49.363	-4.5	-41.360	-4.5	-36.337
-5	-53.102	-5	-43.553	-5	-37.729
-5	-53.102	-5	-43.553	-5	-37.729
-5.25	-55.213	-5.25	-44.710	-5.25	-38.441
-5.5	-57.429	-5.5	-45.904	-5.5	-39.164
-5.75	-59.710	-5.75	-47.130	-5.75	-39.899
-6	-62.026	-6	-48.386	-6	-40.644

-6	-62.026	-6	-48.386	-6	-40.644
-6.5	-66.683	-6.5	-50.984	-6.5	-42.172
-7	-71.318	-7	-53.694	-7	-43.751
-7.5	-75.981	-7.5	-56.526	-7.5	-45.386
-8	-80.865	-8	-59.502	-8	-47.083
-8	-80.865	-8	-59.502	-8	-47.083
-8.25	-83.525	-8.25	-61.061	-8.25	-47.959
-8.5	-86.286	-8.5	-62.661	-8.5	-48.851
-8.75	-89.124	-8.75	-64.295	-8.75	-49.759
-9	-92.021	-9	-65.961	-9	-50.681
-9	-92.021	-9	-65.961	-9	-50.681
-9.5	-97.980	-9.5	-69.380	-9.5	-52.569
-10	-104.237	-10	-72.907	-10	-54.509
-10.5	-111.028	-10.5	-76.550	-10.5	-56.499
-11	-118.759	-11	-80.335	-11	-58.539
-11	-118.759	-11	-80.335	-11	-58.539
-11.25	-123.236	-11.25	-82.302	-11.25	-59.578
-11.5	-127.967	-11.5	-84.298	-11.5	-60.628
-11.75	-132.840	-11.75	-86.306	-11.75	-61.686
-12	-137.752	-12	-88.313	-12	-62.750
-12	-137.752	-12	-88.313	-12	-62.750
-12.5	-147.331	-12.5	-92.265	-12.5	-64.889
-13	-156.063	-13	-96.058	-13	-67.033
-13.5	-163.428	-13.5	-99.612	-13.5	-69.169
-14	-169.020	-14	-102.864	-14	-71.288
-14	-169.020	-14	-102.864	-14	-71.288
-14.25	-171.053	-14.25	-104.361	-14.25	-72.338
-14.5	-172.538	-14.5	-105.767	-14.5	-73.382
-14.75	-173.453	-14.75	-107.079	-14.75	-74.419
-15	-173.783	-15	-108.294	-15	-75.447
-15	-173.783	-15	-108.294	-15	-75.447

-15.25	-173.521	-15.25	-109.411	-15.25	-76.467
-15.5	-172.666	-15.5	-110.431	-15.5	-77.479
-15.75	-171.225	-15.75	-111.354	-15.75	-78.482
-16	-169.212	-16	-112.183	-16	-79.477
-16	-169.212	-16	-112.183	-16	-79.477
-16.33	-165.681	-16.33	-113.148	-16.33	-80.790
-16.67	-161.241	-16.67	-113.962	-16.67	-82.090
-17	-155.956	-17	-114.635	-17	-83.376
-17.33	-149.891	-17.33	-115.178	-17.33	-84.650
-17.33	-149.891	-17.33	-115.178	-17.33	-84.650
-17.67	-143.114	-17.67	-115.605	-17.67	-85.914
-18	-135.695	-18	-115.929	-18	-87.167
-18.33	-127.709	-18.33	-116.164	-18.33	-88.412
-18.67	-119.233	-18.67	-116.325	-18.67	-89.650
-18.6667	-119.233	-18.67	-116.325	-18.67	-89.650
-19	-110.348	-19	-116.425	-19	-90.882
-19.33	-101.146	-19.33	-116.482	-19.33	-92.110
-19.67	-91.730	-19.67	-116.512	-19.67	-93.336
-20	-82.213	-20	-116.530	-20	-94.560

G.2 Three-dimensional Analysis

Table G.2: Lateral Wall Movements of Case 1 after Strut Failure from Three-dimensional Analysis

Case 1A		**Case 1B**		**Case 1C**	
Y	**Ux**	**Y**	**Ux**	**Y**	**Ux**
[m]	**[mm]**	**[m]**	**[mm]**	**[m]**	**[mm]**
0	-19.686	0	-15.891	0	-12.744
-1	-25.618	-1	-19.612	-1	-14.868
-2	-26.553	-2	-22.747	-2	-16.955
-2	-26.553	-2	-22.747	-2	-16.955
-2.25	-27.681	-2.25	-23.573	-2.25	-17.490

-2.5	-29.569	-2.5	-24.487	-2.5	-18.033
-2.5	-29.569	-2.5	-24.487	-2.5	-18.033
-2.75	-30.525	-2.75	-25.318	-2.75	-18.567
-3	-32.243	-3	-26.230	-3	-19.108
-3	-32.243	-3	-26.230	-3	-19.108
-4	-40.690	-4	-30.062	-4	-21.268
-5	-42.862	-5	-33.457	-5	-23.371
-5	-42.862	-5	-33.457	-5	-23.371
-5.25	-44.920	-5.25	-34.634	-5.25	-23.932
-5.5	-48.056	-5.5	-35.964	-5.5	-24.503
-5.5	-48.056	-5.5	-35.964	-5.5	-24.503
-5.75	-49.852	-5.75	-37.138	-5.75	-25.060
-6	-52.554	-6	-38.436	-6	-25.625
-6	-52.554	-6	-38.436	-6	-25.625
-7	-65.006	-7	-43.880	-7	-27.858
-8	-68.813	-8	-48.417	-8	-29.937
-8	-68.813	-8	-48.417	-8	-29.937
-8.25	-71.225	-8.25	-49.864	-8.25	-30.485
-8.5	-74.880	-8.5	-51.470	-8.5	-31.041
-8.5	-74.880	-8.5	-51.470	-8.5	-31.041
-8.75	-77.016	-8.75	-52.851	-8.75	-31.572
-9	-80.056	-9	-54.335	-9	-32.107
-9	-80.056	-9	-54.335	-9	-32.107
-10	-93.677	-10	-60.113	-10	-34.148
-11	-98.220	-11	-64.034	-11	-35.869
-11	-98.220	-11	-64.034	-11	-35.869
-11.25	-101.507	-11.25	-65.201	-11.25	-36.306
-11.5	-106.162	-11.5	-66.482	-11.5	-36.745
-11.5	-106.162	-11.5	-66.482	-11.5	-36.745
-11.75	-109.161	-11.75	-67.459	-11.75	-37.143
-12	-112.760	-12	-68.479	-12	-37.541

-12	-112.760	-12	-68.479	-12	-37.541
-13	-126.524	-13	-71.734	-13	-38.951
-14	-128.846	-14	-71.660	-14	-39.832
-14	-128.846	-14	-71.660	-14	-39.832
-14.25	-128.666	-14.25	-71.306	-14.25	-39.992
-14.5	-128.873	-14.5	-70.946	-14.5	-40.144
-14.5	-128.873	-14.5	-70.946	-14.5	-40.144
-14.75	-128.053	-14.75	-70.342	-14.75	-40.260
-15	-126.942	-15	-69.604	-15	-40.353
-15	-126.942	-15	-69.604	-15	-40.353
-15.5	-123.424	-15.5	-67.658	-15.5	-40.463
-16	-117.095	-16	-65.041	-16	-40.474
-16	-117.095	-16	-65.041	-16	-40.474
-17	-98.925	-17	-58.151	-17	-40.243
-18	-77.080	-18	-49.518	-18	-39.724
-18	-77.080	-18	-49.518	-18	-39.724
-19	-51.696	-19	-39.786	-19	-39.028
-20	-18.732	-20	-28.929	-20	-38.231

Table G.3: Lateral Wall Movements of Case 2 after Strut Failure from Three-dimensional Analysis

Case 2A		**Case 2B**		**Case 2C**	
Y	**Ux**	**Y**	**Ux**	**Y**	**Ux**
[m]	**[mm]**	**[m]**	**[mm]**	**[m]**	**[mm]**
0	-25.287	0	-24.318	0	-30.431
-1	-34.608	-1	-28.763	-1	-32.151
-2	-34.260	-2	-31.920	-2	-33.780
-2	-34.260	-2	-31.920	-2	-33.780
-2.25	-35.425	-2.25	-32.788	-2.25	-34.216
-2.5	-37.946	-2.5	-33.875	-2.5	-34.668
-2.5	-37.946	-2.5	-33.875	-2.5	-34.668

-2.75	-39.205	-2.75	-34.851	-2.75	-35.087
-3	-41.898	-3	-35.996	-3	-35.520
-3	-41.898	-3	-35.996	-3	-35.520
-4	-53.993	-4	-40.725	-4	-37.232
-5	-53.697	-5	-44.094	-5	-38.760
-5	-53.697	-5	-44.094	-5	-38.760
-5.25	-55.795	-5.25	-45.391	-5.25	-39.201
-5.5	-59.801	-5.5	-46.987	-5.5	-39.661
-5.5	-59.801	-5.5	-46.987	-5.5	-39.661
-5.75	-61.798	-5.75	-48.223	-5.75	-40.053
-6	-65.608	-6	-49.721	-6	-40.465
-6	-65.608	-6	-49.721	-6	-40.465
-7	-82.834	-7	-56.086	-7	-42.045
-8	-83.888	-8	-60.257	-8	-43.237
-8	-83.888	-8	-60.257	-8	-43.237
-8.25	-86.423	-8.25	-61.752	-8.25	-43.574
-8.5	-91.186	-8.5	-63.576	-8.5	-43.928
-8.5	-91.186	-8.5	-63.576	-8.5	-43.928
-8.75	-93.813	-8.75	-64.923	-8.75	-44.193
-9	-98.255	-9	-66.534	-9	-44.475
-9	-98.255	-9	-66.534	-9	-44.475
-10	-116.976	-10	-72.937	-10	-45.452
-11	-119.164	-11	-75.910	-11	-45.767
-11	-119.164	-11	-75.910	-11	-45.767
-11.25	-122.799	-11.25	-76.923	-11.25	-45.838
-11.5	-128.678	-11.5	-78.220	-11.5	-45.923
-11.5	-128.678	-11.5	-78.220	-11.5	-45.923
-11.75	-131.860	-11.75	-78.910	-11.75	-45.906
-12	-136.407	-12	-79.819	-12	-45.903
-12	-136.407	-12	-79.819	-12	-45.903
-13	-154.426	-13	-82.879	-13	-45.668

-14	-154.250	-14	-80.748	-14	-44.498
-14	-154.250	-14	-80.748	-14	-44.498
-14.25	-153.744	-14.25	-79.950	-14.25	-44.137
-14.5	-154.196	-14.5	-79.298	-14.5	-43.783
-14.5	-154.196	-14.5	-79.298	-14.5	-43.783
-14.75	-152.809	-14.75	-78.198	-14.75	-43.354
-15	-151.722	-15	-77.039	-15	-42.902
-15	-151.722	-15	-77.039	-15	-42.902
-15.5	-145.971	-15.5	-73.659	-15.5	-41.803
-16	-140.530	-16	-70.674	-16	-40.768
-16	-140.530	-16	-70.674	-16	-40.768
-18	-110.367	-18	-56.084	-18	-35.994
-20	-20.315	-20	-24.208	-20	-28.096

Table G.4: Lateral Wall Movements of Case 3 after Strut Failure from Three-dimensional Analysis

Case 3A		**Case 3B**		**Case 3C**	
Y	**Ux**	**Y**	**Ux**	**Y**	**Ux**
[m]	**[mm]**	**[m]**	**[mm]**	**[m]**	**[mm]**
0	-23.828	0	-23.923	0	-30.486
-1	-34.327	-1	-28.825	-1	-32.341
-2	-33.539	-2	-31.818	-2	-34.045
-2	-33.539	-2	-31.818	-2	-34.045
-2.25	-34.761	-2.25	-32.683	-2.25	-34.491
-2.5	-37.505	-2.5	-33.852	-2.5	-34.963
-2.5	-37.505	-2.5	-33.852	-2.5	-34.963
-2.75	-38.588	-2.75	-34.818	-2.75	-35.404
-3	-41.394	-3	-36.044	-3	-35.870
-3	-41.394	-3	-36.044	-3	-35.870
-4	-54.985	-4	-41.386	-4	-37.758
-5	-53.833	-5	-44.514	-5	-39.385

-5	-53.833	-5	-44.514	-5	-39.385
-5.25	-55.907	-5.25	-45.724	-5.25	-39.837
-5.5	-60.163	-5.5	-47.340	-5.5	-40.323
-5.5	-60.163	-5.5	-47.340	-5.5	-40.323
-5.75	-61.883	-5.75	-48.524	-5.75	-40.747
-6	-65.703	-6	-50.088	-6	-41.206
-6	-65.703	-6	-50.088	-6	-41.206
-7	-84.164	-7	-57.095	-7	-43.051
-8	-84.103	-8	-60.827	-8	-44.428
-8	-84.103	-8	-60.827	-8	-44.428
-8.25	-86.595	-8.25	-62.190	-8.25	-44.809
-8.5	-91.629	-8.5	-64.024	-8.5	-45.228
-8.5	-91.629	-8.5	-64.024	-8.5	-45.228
-8.75	-93.977	-8.75	-65.288	-8.75	-45.559
-9	-98.380	-9	-66.944	-9	-45.930
-9	-98.380	-9	-66.944	-9	-45.930
-10	-118.191	-10	-73.961	-10	-47.354
-11	-119.458	-11	-76.441	-11	-48.029
-11	-119.458	-11	-76.441	-11	-48.029
-11.25	-123.146	-11.25	-77.352	-11.25	-48.206
-11.5	-129.377	-11.5	-78.702	-11.5	-48.422
-11.5	-129.377	-11.5	-78.702	-11.5	-48.422
-11.75	-132.364	-11.75	-79.334	-11.75	-48.523
-12	-136.912	-12	-80.315	-12	-48.665
-12	-136.912	-12	-80.315	-12	-48.665
-13	-156.340	-13	-84.091	-13	-49.113
-14	-155.850	-14	-81.674	-14	-48.516
-14	-155.850	-14	-81.674	-14	-48.516
-14.25	-155.450	-14.25	-80.883	-14.25	-48.320
-14.5	-156.313	-14.5	-80.411	-14.5	-48.159
-14.5	-156.313	-14.5	-80.411	-14.5	-48.159

-14.75	-155.091	-14.75	-79.418	-14.75	-47.915
-15	-154.183	-15	-78.396	-15	-47.655
-15	-154.183	-15	-78.396	-15	-47.655
-15.5	-150.387	-15.5	-75.811	-15.5	-47.034
-16	-142.653	-16	-72.378	-16	-46.280
-16	-142.653	-16	-72.378	-16	-46.280
-17	-120.574	-17	-63.763	-17	-44.467
-18	-94.430	-18	-53.387	-18	-42.241
-18	-94.430	-18	-53.387	-18	-42.241
-19	-66.927	-19	-42.358	-19	-39.828
-20	-22.743	-20	-28.673	-20	-37.124

Appendix H: Earth Pressure on the Primary Wall after Lowest Strut Failure Condition

H.1 Charts of Lateral Earth Pressure after Strut Failure

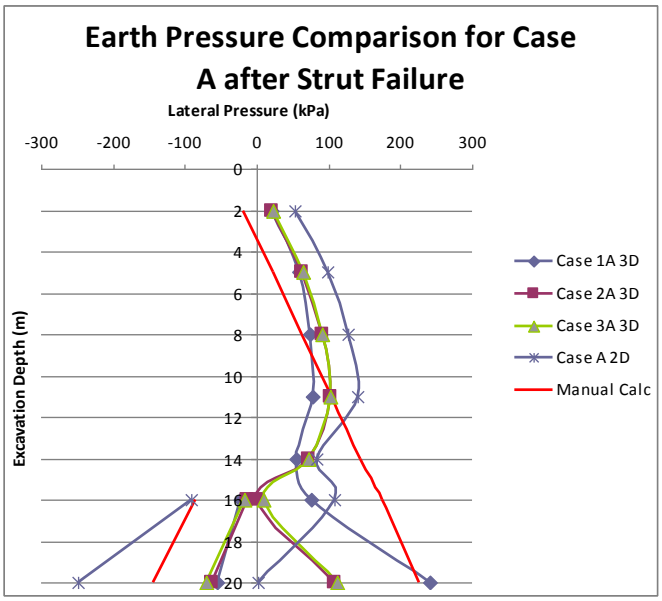

Figure H.1: Lateral Earth Pressure Diagram for Cases of Flexible Wall after Strut Failure

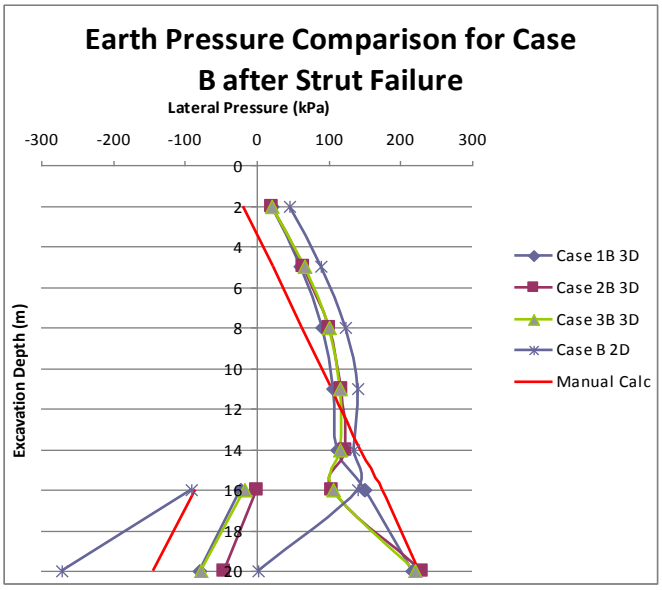

Figure H.2: Lateral Earth Pressure Diagram for Cases of Medium Flexible Wall after Strut Failure

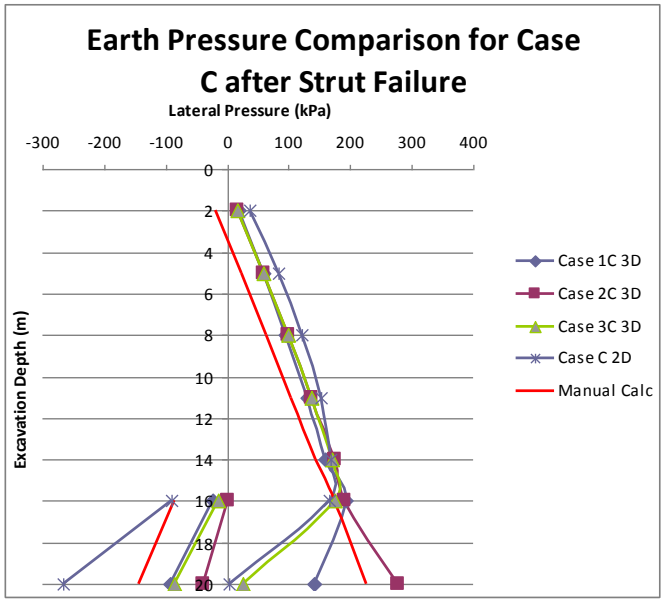

Figure H.3: Lateral Earth Pressure Diagram for Cases of Stiff Wall after Strut Failure

H.2 Tables of Lateral Earth Pressure

The tables of lateral earth pressure for strut failure condition from plane strain and three-dimensional analysis are presented on the next pages.

Table H.1: Lateral Earth Pressure for Strut Failure Condition from Plane Strain Analysis

Case A			**Case B**			**Case C**			**Lateral Pressure from Manual Calculations***
Active Pressure			**Active Pressure**			**Active Pressure**			
Stress Points No	**Y**	**s' xx**	**Stress Points No**	**Y**	**s' xx**	**Stress Points No**	**Y**	**s' xx**	
	[m]	**[kN/m^2]**		**[m]**	**[kN/m^2]**		**[m]**	**[kN/m^2]**	**[kN/m^2]**
3195	-2.157	52.979	3603	-1.968	45.171	3195	-2.157	36.785	-10.658
3543	-5.010	98.856	3543	-5.010	89.980	3543	-5.010	82.848	28.131
3482	-9.061	127.546	3483	-7.998	123.666	3483	-7.998	121.891	83.228
3507	-10.953	140.559	3507	-10.953	141.263	3507	-10.953	151.661	108.967
3147	-14.118	83.622	3423	-13.925	135.136	3423	-13.925	167.131	152.001
3398	-16.049	107.447	3398	-16.049	141.268	3398	-16.049	166.778	178.261
3207	-19.916	2.308	3207	-19.916	1.406	3207	-19.916	3.172	230.856
Passive Pressure			**Passive Pressure**			**Passive Pressure**			**Lateral Pressure from Manual Calculations***
Stress Points No	**Y**	**s' xx**	**Stress Points No**	**Y**	**s' xx**	**Stress Points No**	**Y**	**s' xx**	
	[m]	**[kN/m^2]**		**[m]**	**[kN/m^2]**		**[m]**	**[kN/m^2]**	**[kN/m^2]**
7803	-16.084	-90.4692	7803	-16.084	-79.948	7803	-16.084	-90.8481	-79.948
7778	-19.916	-248.623	7778	-19.916	-150.452	7778	-19.916	-266.092	-150.452

*based on Y from Case A and Case C

Table H.2: Lateral Earth Pressure for Strut Failure Condition of Case 1 from Three-dimensional Analysis

Case 1A			**Case 1B**			**Case 1C**			**Lateral Pressure from Manual Calculations**
Active Pressure			**Active Pressure**			**Active Pressure**			
Stress Points No	**Y**	**σ_3'**	**Stress Points No**	**Y**	**σ_3'**	**Stress Points No**	**Y**	**σ_3'**	
	[m]	**[kN/m^2]**		**[m]**	**[kN/m^2]**		**[m]**	**[kN/m^2]**	**[kN/m^2]**
73	-1.577	20.962	85	-1.577	20.118	73	-1.577	17.676	-18.548
8317	-4.577	58.010	8401	-4.577	60.798	8317	-4.577	58.415	22.252
16561	-7.577	74.526	16717	-7.577	90.493	16561	-7.577	95.494	63.052
24805	-10.577	77.032	25033	-10.577	105.729	24805	-10.577	129.274	103.852
33049	-13.577	55.279	33349	-13.577	111.622	33049	-13.577	158.442	144.652
41293	-15.789	76.076	41665	-15.789	149.054	41293	-15.789	193.060	174.726
46789	-19.577	240.721	47209	-19.577	216.254	46789	-19.577	141.631	226.252
Passive Pressure			**Passive Pressure**			**Passive Pressure**			**Lateral Pressure from Manual Calculations**
Stress Points No	**Y**	**σ_3'**	**Stress Points No**	**Y**	**σ_3'**	**Stress Points No**	**Y**	**σ_3'**	
	[m]	**[kN/m^2]**		**[m]**	**[kN/m^2]**		**[m]**	**[kN/m^2]**	**[kN/m^2]**
46696	-16.423	-21.849	47104	-16.423	-22.072	46696	-16.423	-23.027	-86.177
49441	-19.577	-55.098	49873	-19.577	-80.265	49441	-19.577	-91.916	-144.223

Table H.3: Lateral Earth Pressure for Strut Failure Condition of Case 2 from Three-dimensional Analysis

Case 2A			**Case 2B**			**Case 2C**			**Lateral Pressure from Manual Calculations**
Active Pressure			**Active Pressure**			**Active Pressure**			
Stress Points No	**Y**	**σ_3'**	**Stress Points No**	**Y**	**σ_3'**	**Stress Points No**	**Y**	**σ_3'**	
	[m]	**[kN/m^2]**		**[m]**	**[kN/m^2]**		**[m]**	**[kN/m^2]**	**[kN/m^2]**
39	-1.577	21.694	39	-1.577	20.800	39	-1.577	17.389	-18.548
5619	-4.577	62.293	5619	-4.577	64.426	5619	-4.577	59.660	22.252
11199	-7.577	91.872	11199	-7.577	100.147	11199	-7.577	99.770	63.052
16779	-10.577	102.428	16779	-10.577	117.564	16779	-10.577	137.305	103.852
22359	-13.577	71.273	22359	-13.577	122.689	22359	-13.577	174.473	144.652
27939	-15.789	0.000	27939	-15.789	105.323	27939	-15.789	191.396	174.726
29799	-19.155	108.713	29799	-19.155	229.539	29799	-19.155	276.524	220.504
Passive Pressure			**Passive Pressure**			**Passive Pressure**			**Lateral Pressure from Manual Calculations**
Stress Points No	**Y**	**σ_3'**	**Stress Points No**	**Y**	**σ_3'**	**Stress Points No**	**Y**	**σ_3'**	
	[m]	**[kN/m^2]**		**[m]**	**[kN/m^2]**		**[m]**	**[kN/m^2]**	**[kN/m^2]**
31620	-16.845	-12.356	31620	-16.845	0.000	31620	-16.845	0.000	-93.954
31615	-19.155	-63.042	31615	-19.155	-44.666	31615	-19.155	-40.170	-136.446

Table H.4: Lateral Earth Pressure for Strut Failure Condition of Case 3 from Three-dimensional Analysis

Case 3A			**Case 3B**			**Case 3C**			**Lateral Pressure from Manual Calculations**
Active Pressure			**Active Pressure**			**Active Pressure**			
Stress Points No	**Y**	**σ_3'**	**Stress Points No**	**Y**	**σ_3'**	**Stress Points No**	**Y**	**σ_3'**	
	[m]	**[kN/m^2]**		**[m]**	**[kN/m^2]**		**[m]**	**[kN/m^2]**	**[kN/m^2]**
27	-1.577	22.853	27	-1.577	21.096	27	-1.577	17.058	-18.548
5499	-4.577	63.626	5499	-4.577	66.297	5499	-4.577	59.971	22.252
10971	-7.577	91.356	10971	-7.577	100.494	10971	-7.577	100.008	63.052
16443	-10.577	102.113	16443	-10.577	115.857	16443	-10.577	137.048	103.852
21915	-13.577	71.205	21915	-13.577	116.634	21915	-13.577	170.769	144.652
27387	-15.789	9.096	27387	-15.789	106.098	27387	-15.789	175.203	174.726
31035	-19.577	112.794	31035	-19.577	220.706	31035	-19.577	24.583	226.252
Passive Pressure			**Passive Pressure**			**Passive Pressure**			**Lateral Pressure from Manual Calculations**
Stress Points No	**Y**	**σ_3'**	**Stress Points No**	**Y**	**σ_3'**	**Stress Points No**	**Y**	**σ_3'**	
	[m]	**[kN/m^2]**		**[m]**	**[kN/m^2]**		**[m]**	**[kN/m^2]**	**[kN/m^2]**
31006	-16.423	-16.421	31006	-16.423	-16.370	31006	-16.423	-15.055	-86.177
32827	-19.577	-70.438	32827	-19.577	-78.571	32827	-19.577	-85.612	-144.223

Appendix I: Percentages of Strut Forces Distribution after Lowest Strut Failure Condition

The strut forces before and after the lowest strut failure are tabulated in *Tables I.1, I.2* and *I.3* below. All of the results are from three-dimensional models.

In these tables, T refers to the strut immediately above, D refers to the strut immediately on the top diagonal, and S refers to the strut immediately on the left or right side of the failed strut. Please note that for D strut and S strut in *Tables I.1, I.2* and *I.3* refer to each strut, either on the right or left hand side of the failed strut.

Table I.1: Strut Forces Before and After Lowest Strut Failure of Case 1

Case 1A				
Strut forces of the failed strut	595.573 kN			
At the end of excavation process				
Strut Forces	**Before**	**After**	**Add. Force**	**Dist. from Failed Strut**
	(kN)	**(kN)**	**(%)**	**(%)**
T	1712.260	1944.572	13.568	39.007
D	1622.489	1662.502	2.466	6.718
S	582.080	688.481	18.279	17.865
Case 1B				
Strut forces of the failed strut	564.949 kN			
At the end of excavation process				
Strut Forces	**Before**	**After**	**Add. Force**	**Dist. from Failed Strut**
	(kN)	**(kN)**	**(%)**	**(%)**
T	1772.018	2056.172	16.036	47.711
D	1566.581	1595.150	1.824	4.797

S	502.780	549.335	9.260	7.817
Case 1C				
Strut forces of the failed strut	653.489 kN			
At the end of excavation process				
Strut Forces	**Before**	**After**	**Add. Force**	**Dist. from Failed Strut**
	(kN)	**(kN)**	**(%)**	**(%)**
T	1849.928	2091.286	13.047	40.525
D	1275.518	1320.016	3.489	7.471
S	449.447	532.802	18.546	13.996

Table I.2: Strut Forces Before and After Lowest Strut Failure of Case 2

Case 2A				
Strut forces of the failed strut	632.149 kN			
At the end of excavation process				
Strut Forces	**Before**	**After**	**Add. Force**	**Dist. from Failed Strut**
	(kN)	**(kN)**	**(%)**	**(%)**
T	1935.772	2181.036	12.670	38.798
D	1946.015	2003.423	2.950	9.081
S	637.772	733.688	15.039	15.173
Case 2B				
Strut forces of the failed strut	493.947 kN			
At the end of excavation process				
Strut Forces	**Before**	**After**	**Add. Force**	**Dist. from Failed Strut**
	(kN)	**(kN)**	**(%)**	**(%)**
T	1787.172	2040.150	14.155	51.216
D	1801.218	1837.742	2.028	7.394
S	490.506	507.008	3.364	3.341

Case 2C				
Strut forces of the failed strut	387.601 kN			
At the end of excavation process				
Strut Forces	**Before**	**After**	**Add. Force**	**Dist. from Failed Strut**
	(kN)	**(kN)**	**(%)**	**(%)**
T	1446.242	1571.586	8.667	32.338
D	1449.017	1470.673	1.495	5.587
S	382.103	409.958	7.290	7.187

Table I.3: Strut Forces Before and After Lowest Strut Failure of Case 3

Case 3A				
Strut forces of the failed strut	624.889 kN			
At the end of excavation process				
Strut Forces	**Before**	**After**	**Add. Force**	**Dist. from Failed Strut**
	(kN)	**(kN)**	**(%)**	**(%)**
T	2018.472	2266.190	12.273	39.642
D	2049.146	2110.582	2.998	9.831
S	630.961	734.650	16.434	16.593
Case 3B				
Strut forces of the failed strut	535.052 kN			
At the end of excavation process				
Strut Forces	**Before**	**After**	**Add. Force**	**Dist. from Failed Strut**
	(kN)	**(kN)**	**(%)**	**(%)**
T	1786.858	2048.826	14.661	48.961
D	1793.282	1829.258	2.006	6.724
S	540.321	564.752	4.522	4.566
Case 3C				

Strut forces of the failed strut	532.907 kN			
At the end of excavation process				
Strut Forces	**Before**	**After**	**Add. Force**	**Dist. from Failed Strut**
	(kN)	**(kN)**	**(%)**	**(%)**
T	1720.572	1897.618	10.290	33.223
D	1770.586	1802.949	1.828	6.073
S	563.870	615.568	9.168	9.701